Department of Radio Science and Engineering

Compact UHF-band antennas for mobile terminals: focus on modelling, implementation, and user interaction

Jari Holopainen

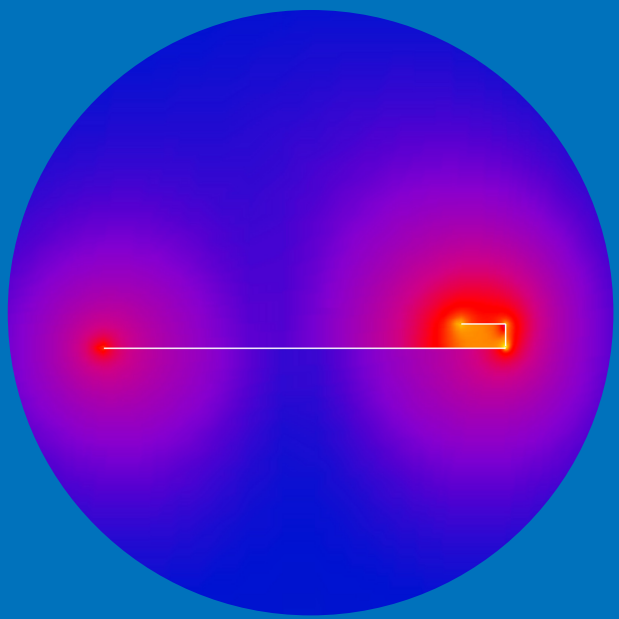

Aalto University

DOCTORAL DISSERTATIONS

Aalto University publication series
DOCTORAL DISSERTATIONS 28/2011

Compact UHF-band antennas for mobile terminals: focus on modelling, implementation, and user interaction

Jari Holopainen

Doctoral dissertation for the degree of Doctor of Science in Technology to be presented with due permission of the School of Electrical Engineering for public examination and debate in Auditorium S4 at the Aalto University School of Electrical Engineering (Espoo, Finland) on the 29th of April 2011 at 12 noon.

Aalto University
School of Electrical Engineering
Department of Radio Science and Engineering

Supervisor
Prof., D.Sc. (Tech.) Pertti Vainikainen

Instructor
D.Sc. (Tech.) Outi Kivekäs

Preliminary examiners
Prof. Ph.D. (Doctor of Eng.), Koichi Ito, Chiba University, Japan
Ph.D. (E.E.), Ping Hui, Nokia Corporation, Canada

Opponents
Prof. Dr.-Ing Dirk Manteuffel, Christian-Albrechts-Universitet, Kiel, Germany
Ph.D. Kevin Boyle, EPCOS UK Limited, United Kingdom

Aalto University publication series
DOCTORAL DISSERTATIONS 28/2011

ISBN 978-952-60-4086-8 (pdf)
ISBN 978-952-60-4085-1 (printed)
ISSN-L 1799-4934
ISSN 1799-4942 (pdf)
ISSN 1799-4934 (printed)

Aalto Print
Helsinki 2011

The dissertation can be read at http://lib.tkk.fi/Diss/

Aalto University

Abstract

Aalto University, P.O. Box 11000, FI-00076 Aalto www.aalto.fi

Author
Jari Holopainen

Name of the doctoral dissertation
Compact UHF-band antennas for mobile terminals: focus on modelling, implementation, and user interaction

Publisher School of Electrical Engineering

Unit Department of Radio Science and Engineering

Series Aalto University publication series DOCTORAL DISSERTATIONS 28/2011

Field of research Radio Engineering

Manuscript submitted 29 November 2010 **Manuscript revised** 10 March 2011

Date of the defence 29 April 2011 **Language** English

☐ **Monograph** ☒ **Article dissertation (summary + original articles)**

The background of this thesis is the trend of ever decreasing space available for antennas embedded within mobile terminals. At the same time the antennas are increasingly required to cover a large number of separate frequency bands and/or have wideband operation. In addition, those antennas should perform sufficiently well in the vicinity of the user. This forms the motivation for the novel compact coupling-based antennas introduced and studied in this thesis.

The operation of the compact coupling antennas is based on exploiting the separate wavemodes supported by the chassis of the mobile terminal. The antenna element itself functions mainly as a coupler which couples to those chassis wavemodes. That is the reason why they are called coupling-based antennas. This work concentrates on the modelling, implementation and design of such antennas in free space, and the effect of the user on the operation of the antenna. The understanding gained in this thesis can be exploited in the development of the antennas for mobile terminals of the future.

In the first part of the thesis, an equivalent circuit model is derived for a capacitive coupling-based antenna. This model gives a helpful physical explanation for the operation of this type of antennas. Broadband small antennas operating in the lower part of the UHF band are also implemented and analysed in detail. These kinds of antennas could find applications, for example, in digital television reception, low-band LTE, or the spectrum sensing of cognitive radios. Furthermore, it is shown that very low-profile antennas can be implemented by exciting the chassis wavemodes galvanically with a direct feed. The implementation of frequency-tuneable antennas is also studied in order to cover broad virtual bandwidth or several separate non-simultaneous frequency bands. The second part of this thesis discusses issues concerning user interaction with the coupling-based antennas. The antenna-user interaction is first modelled with an equivalent circuit which provides an improved understanding of the phenomenon. Then, the effects of the user's hands on the operation of the broadband lower UHF-band antenna is studied in detail. In the end of the thesis, a method for reshaping the near fields of the mobile terminal antenna is also proposed, for example, for improved hearing-aid compatibility.

Keywords capacitive coupling element, digital television, direct feed, equivalent circuits, hearing-aid compatibility, mobile antennas, receiving antennas, frequency-tuneable antennas, user effect

ISBN (printed) 978-952-60-4085-1 **ISBN (pdf)** 978-952-60-4086-8

ISSN-L 1799-4934 **ISSN (printed)** 1799-4934 **ISSN (pdf)** 1799-4942

Location of publisher Espoo **Location of printing** Helsinki **Year** 2011

Pages 86 **The dissertation can be read at** http://lib.tkk.fi/Diss/

Aalto-yliopisto

Tiivistelmä

Aalto-yliopisto, PL 11000, 00076 Aalto www.aalto.fi

Tekijä
Jari Holopainen

Väitöskirjan nimi
Kompaktien UHF-taajuuskaistalla toimivien matkapuhelinantennien mallinnus ja suunnittelu sekä käyttäjän vaikutus antennien toimintaan

Julkaisija sähkötekniikan korkeakoulu

Yksikkö radiotieteen ja -tekniikan laitos

Sarja Aalto University publication series DOCTORAL DISSERTATIONS 28/2011

Tutkimusala radiotekniikka

Käsikirjoituksen pvm 29.11.2010 **Korjatun käsikirjoituksen pvm** 10.03.2011

Väitöspäivä 29.04.2011 **Kieli** Englanti

☐ **Monografia** ☒ **Yhdistelmäväitöskirja (yhteenveto-osa + erillisartikkelit)**

Tiivistelmä

Antenneille varattu tila matkapuhelimen sisällä pienenee jatkuvasti. Tästä huolimatta antenneilta vaaditaan usein toimimista laajalla tai usealla erillisellä taajuuskaistalla. Lisäksi antennien tulee toimia riittävän hyvin myös käyttäjän läheisyydessä. Nämä seikat muodostavat lähtökohdan tälle tutkimukselle.

Tutkimuksessa kehitettyjen antennien toiminta perustuu päätelaitteen rungon hyödyntämiseen pääasiallisena säteilijänä. Varsinaisen antennielementin tehtävänä on kytkeä säteilevät sähkövirrat laitteen runkoon. Työssä keskitytään näiden antennirakenteiden toiminnan mallintamiseen ja suunnitteluun sekä ymmärtämään, miten käyttäjä vaikuttaa antennin toimintaan. Saavutettua osaamista voidaan hyödyntää ja soveltaa eri matkaviestinjärjestelmien päätelaiteantennien suunnittelussa.

Työn ensimmäisessä osassa johdetaan sähköinen vastinpiirimalli antennien toiminnan ymmärtämiseksi. Lisäksi siinä toteutetaan pieni laajakaistainen UHF-taajuusalueella toimiva vastaanottoantenni, jota voidaan käyttää esimerkiksi digitaalitelevision signaalin vastaanotossa. Samantyyppistä antennia voidaan soveltaa myös esimerkiksi LTE-järjestelmässä tai radiospektrin havainnoinnissa kognitiivisessa radiossa. Passiivisten laajakaista-antennien lisäksi työssä tutkitaan taajuusviritettäviä antenneja, joilla voidaan toteuttaa laajoja virtuaalisia kaistanleveyksiä tai useita erillisiä taajuuskaistoja yhtä antennielementtiä käyttäen. Lisäksi työssä osoitetaan, että antennin kokoa voidaan pienentää huomattavasti herättämällä rungon säteilevät virrat galvaanisen suorasyöttökytkennän avulla. Työn toisessa osassa käsitellään käyttäjän vaikutusta antennin toimintaan. Aluksi ilmiötä mallinnetaan ja selitetään sähköisen vastinpiirin avulla. Tämän jälkeen tutkitaan laajakaistaisen UHF-taajuuskaistalla toimivan vastaanottoantennin toimintaa laitteen ollessa käyttäjän käsissä. Lopuksi työssä esitetään menetelmä, jolla matkapuhelinantennin lähikenttiä saadaan muokattua siten, että käyttäjän mahdollisen kuulolaitteen toiminta ei häiriinny puhelimen toiminnasta.

Avainsanat kapasitiivinen kytkentäelementti, kuulolaiteyhteensopivuus, käyttäjän vaikutus, matkapuhelinantennit, mobiilitelevisio, suorasyöttöantennit, sähköiset vastinpiirit, taajuusviritettävät antennit, vastaanottoantennit

ISBN (painettu) 978-952-60-4085-1 **ISBN (pdf)** 978-952-60-4086-8

ISSN-L 1799-4934 **ISSN (painettu)** 1799-4934 **ISSN (pdf)** 1799-4942

Julkaisupaikka Espoo **Painopaikka** Helsinki **Vuosi** 2011

Sivumäärä 86 **Luettavissa verkossa osoitteessa** http://lib.tkk.fi/Diss/

Acknowledgement

Firstly, I want to thank Professor Dr. Pertti Vainikainen for providing a very interesting research topic for my thesis and for his kind supervision, and especially sharing his extensive experience in small antennas and academic work.

My instructors Dr. Outi Kivekäs, Dr. Clemens Icheln, and Dr. Juha Villanen deserve my deepest gratitude for providing everyday help and support.

My closest working colleagues Mr. Janne Ilvonen and Mr. Risto Valkonen, you have been priceless help in work, and also very good company for creating nice atmosphere in our antenna team. Other colleagues in the department of radio science and engineering deserve warm thanks, too.

Mr. William Martin performed the English language examination and provided good comments for improving the language of my thesis. I am very grateful for his work.

During my doctoral studies I also spent three months (July-August 2009) in the University of Birmingham, United Kingdom. Professor Dr. Peter Hall, thank you for sharing Your great experience with me.

I want to also thank the pre-examiners, Prof. Dr. Koichi Ito and Dr. Ping Hui, for their constructive comments.

In the end, I want to also thank the teachers in Siilinjärvi high school in the years 1996-1999: you have been greatly involved in creating my interest and enthusiasm for the natural science and engineering.

Vantaa, April 7, 2011

Jari Holopainen

Contents

List of publications

This thesis consists of this summary and the following articles which are referred to in the text by their Roman numerals.

[**I**] J. Holopainen, R. Valkonen, O. Kivekäs, J. Ilvonen, and P. Vainikainen, "Broadband Equivalent Circuit Model for Capacitive Coupling Element – Based Mobile Terminal Antenna," *IEEE Antennas and Wireless Propagation Letters,* vol. 9, 2010, pp. 716-719.

[**II**] J. Holopainen, O. Kivekäs, C. Icheln, and P. Vainikainen, "Internal Broadband Antennas for Digital Television Receiver in Mobile Terminals," *IEEE Transactions on Antennas and Propagation*, vol. 58, no. 10, October 2010, pp. 3363-3374.

[**III**] R. Valkonen, J. Holopainen, C. Icheln, and P. Vainikainen, "Minimization of power loss and distortion in a tuning circuit for a mobile terminal antenna," *ISAP 2008 International Symposium on Antennas and Propagation*, Taipei, Taiwan, 27-30 October 2008, pp. 449-452.

[**IV**] J. Holopainen, J. Villanen, C. Icheln, P. Vainikainen, "Mobile terminal antennas implemented by using direct coupling," *EuCAP 2006 1st European Conference on Antennas & Propagation*, Nice, France, 6-10 November 2006, CD-ROM SP-626 (92-9092-937-5), paper: OA17 349858jh.pdf.

[**V**] J. Holopainen, J. Villanen, R. Valkonen, J. Poutanen, O. Kivekäs, C. Icheln, and P. Vainikainen, "Mobile terminal antennas implemented using optimized direct feed," *iWAT 2009 IEEE International Workshop on Antenna Technology*, Santa Monica, California, USA, 2-4 March 2009, paper: PS202.

[**VI**] J. Holopainen, R. Valkonen, J. Ilvonen, O. Kivekäs, L. Martinez, P. Vainikainen, J. R. Kelly, and P. S. Hall, "Equivalent Circuit Model–Based Approach on the User Body Effect of a Mobile Terminal Antenna," *IEEE Loughborough Antennas & Propagation Conference 2010,* Loughborough, UK, 8-9 November 2010, pp. 217-220.

[**VII**] J. Holopainen, O. Kivekäs, J. Ilvonen, R. Valkonen, C. Icheln, and P. Vainikainen, "Effect of the User on the Operation of Lower UHF-Band Mobile Terminal Antennas: Focus on Digital Television Receiver," *IEEE Transactions on Electromagnetic Compatibility*, vol. 53, to be published in a future issue,11 p.

[**VIII**] J. Holopainen, J. Ilvonen, O. Kivekäs, R. Valkonen, C. Icheln, and P. Vainikainen, “Near Field Control of Handset Antennas Based on Inverted Top Wavetraps: Focus on Hearing-Aid Compatibility,” *IEEE Antennas and Wireless Propagation Letters*, vol. 8, 2009, pp. 592-595.

Author's contribution

Prof. Dr. Pertti Vainikainen supervised all the papers. D.Sc. (Tech.) Outi Kivekäs and D.Sc. (Tech.) Clemens Icheln worked as instructors.

The author had the main responsibility for developing the idea and content, and writing paper [**I**]. Mr. Risto Valkonen participated in the development of the idea and content, validation of the proposed circuit model, and in the writing of the paper.

Paper [**II**] is based on long-term research the author has done during his doctoral studies with lower UHF-band receiver antennas, and he had a leading role in developing and writing of the whole paper.

Mr. Risto Valkonen had a leading role in developing and writing paper [**III**]. The author participated in developing the idea and content of the paper. He also had the responsibility for the measurement system for the distortion measurements, and in the writing of the paper.

The author had the main responsibility for developing the idea, content and writing of paper [**IV**].

The idea for paper [**V**] originates from the results of paper [**IV**]. The author participated in developing the antenna structure and had the main responsibility for preparing the paper. Mr. Risto Valkonen participated in the writing of the paper.

The author had the main responsibility for developing the idea, content and writing of paper [**VI**]. Mr. Risto Valkonen participated in the development of the results, and writing of the paper.

Paper [**VII**] is a continuation of paper [**II**]. The author had the main responsibility for developing the research methods, content and writing of the paper. Mr. Janne Ilvonen participated in the simulations and measurements.

The idea for paper [**VIII**] was found by the author and Mr. Janne Ilvonen, who also conducted the simulations. The author had the main responsibility for analysing the results and preparation of the paper. Mr. Janne Ilvonen participated in this preparation work.

List of abbreviations

ACE	Antenna Center of Excellence (European antenna research community)
CCE	Capacitive Coupling Element
DC	Direct Current
DF	Direct Feed
DTV	Digital Television
DVB-H	Digital Video Broadcasting – Handheld standard
EM	Electromagnetic
EMC	Electromagnetic Compatibility
GPS	(Navstar) Global Positioning System
GSM	Global System for Mobile communications (formerly called Groupe Spécial Mobile)
HAC	Hearing-Aid Compatibility
ICNIRP	International Commission on Non-Ionizing Radiation Protection
IEEE	Institute of Electrical and Electronics Engineers
IFA	Inverted-F Antenna
ILA	Inverted-L Antenna
IMD_3	Intermodulation Distortion of the third harmonic
LTCC	Low-Temperature Co-fired Ceramic
MEMS	Micro-Electro-Mechanical System
LTE	Long Term Evolution (advanced 3G technology)
OTA	Over-The-Air
PCB	Printed Circuit Board
PEC	Perfect Electric Conductor
PHEMT	Pseudomorphic High Electron Mobility Transistor
PIFA	Planar Inverted-F Antenna
RF	Radio Frequency

RLC	Resistor-Inductor-Capacitor
SAR	Specific Absorption Rate
SAW	Surface Acoustic Wave
SPDT	Single Pole, Double Throw
SPNT	Single Pole, *N* Throw
TE	Transversal Electric field
TM	Transversal Magnetic field
UHF	Ultra High Frequency band (0.3 – 3 GHz)
WLAN	Wireless Local Area Network
3G	3rd Generation, technology for mobile phones and telecommunication
4G	4th Generation, technology for mobile phones and telecommunication beyond 3G

List of symbols

a	radius of a sphere enclosing an antenna
B_r	relative bandwidth
C	capacitance/capacitor
c	speed of light
D	directivity
d	distance
E	strength of electric field
f_r	resonant frequency
G	gain (electromagnetic)
G_{real}	realised gain
H	strength of magnetic field
h	height
k	impedance scaling factor of an ideal transformer
k_o	wave number in free space
L	inductance/inductor
L_{retn}	return loss
l	length
P	dissipated power
Q	quality factor
Q_o	unloaded quality factor
Q_{rad}	radiation quality factor
Q_d	quality factor for dielectric losses
Q_c	quality factor for conductor losses
R	resistance/resistor
S	maximum acceptable voltage standing wave ratio
T	coupling coefficient
$VSWR$	voltage standing wave ratio
W	stored energy

w	width
X	reactance
Z	impedance
ε_r	relative permittivity (complex)
ε_r'	real part of relative permittivity
ε_r''	imaginary part of relative permittivity
ε_o	permittivity in free space
η_m	matching efficiency
η_{tot}	total efficiency
η_{rad}	radiation efficiency
θ	elevation angle in standard spherical coordinate system
λ_o	wavelength in free space
ρ	reflection coefficient
ρ_d	mass density
σ_{eff}	effective conductivity
φ	azimuth angle in standard spherical coordinate system
ω_r	angular resonant frequency

1. Introduction

1.1. Background

An antenna is a device that transmits and receives radio waves; in transmission an antenna converts a guided wave into a free space wave, and in reception vice versa. Thus, the antenna is a necessary part of all radio systems. The antenna is typically also the largest-sized component of a radio system. The used antenna type depends on the application and the environment where the particular radio system is used. For example, in the typical broadcast field strength a simple conducting wire might be a proper receiving antenna, but in satellite communication systems highly directive parabolic antennas are typically required to be able to separate the wanted signal from the unwanted signals and noise. The most important electrical characteristics of antennas are directional pattern, polarisation, efficiency, and matching. In addition, the mechanical characteristics such as size, shape, weight, and robustness are important, and of course, in mass production also the price and manufacturability are essential. In modern mobile communications devices the antennas operate in a fairly complex and size-limited environment and thus the requirements, especially for the size and shape of the antennas, are very strict.

In order to be an efficient antenna, the length of the radiator structure needs to be at least about a quarter of the wavelength. As the wavelength below 1 GHz is over 300 mm, it is very challenging to implement quarter-wavelength-long radiators within typical mobile terminals whose size is only 100–130 mm. On the other hand, the use of such long wavelengths (low frequencies) is tempting since longer radio waves propagate essentially better than remarkably shorter waves (higher frequencies such as several GHz). Thus, the limited space available for the antennas within mobile devices together with the use of relatively long waves leads to the use of electrically small antennas, whose inherent property is the impaired performance compared to essentially larger antennas. In addition, any “universal” wideband antenna, which would cover simultaneously all the required frequency bands, cannot be implemented. Mobile terminal antennas are hence designed by optimising especially the size, shape and performance of the antenna according to the respective platform, requested frequency band(s), and the performance requirements of the given radio system.

In addition to the inherently suffered performance of electrically small antennas, the user of a handheld mobile device typically affects the

operation of the antennas by additionally impairing the performance. This makes the operation conditions of the antennas ever trickier, and in the worst case the wireless connection can even be blocked due to the user effect. However, users nevertheless assume that any system operates reliably regardless of the holding position and operating location of the mobile device. This problem can be partly overcome with careful design of the antenna system (including possible compensation methods) and by taking into account the realistic performance of the antenna already in the planning procedure of the whole radio system.

During the last decade there has been a significant increase in the number of different functions and radio systems supported by handheld devices. Today's terminals need to cover several separate frequency bands which all need an antenna preferably embedded within the device. The number of the supported frequency bands can still be expected to increase [1], and thus novel antenna solutions are required to be able to cover all the possible frequency bands with sufficiently small and thin antenna structures and adequate performance. In future, more efficient exploitation of the available radio spectrum will probably lead to the concept of cognitive radio, in which the whole radio environment is actively monitored and the radio system dynamically adapts its spectral operation based on the available networks and the needs of the user. Such adaptivity is necessary for covering the increasing number of frequency bands, and particularly for the increasing levels of wireless data traffic. This function requires ever more flexible wideband antennas, especially in the UHF band (0.3-3 GHz) [2].

1.2. Objective of the thesis

The results of this thesis aim at improved understanding of the UHF-band antennas in handheld mobile devices. Especially, the equivalent circuit modelling, implementation, design, and the user body effect of the antennas are handled. Even though the current radio systems and standards, especially the lower UHF-band digital television receiver (DVB-H), are used as application examples, the understanding gained in this thesis can be seen as system-independent and long-term, and it can be exploited for designing the mobile terminal antennas operating in the UHF band, for instance, for low-band LTE, future 4G and cognitive radios.

1.3. Organisation of the thesis

The main scientific results of this thesis are presented in articles [**I**]-[**VIII**]. The thesis is divided into two main parts. The first part handles the operation and implementation of the compact coupling-based antennas in

free space [**I**]-[**V**], and the second part is devoted for the user-interaction issues of the studied antennas [**VI**]-[**VIII**]. The order of the articles within each part is chosen in such a way that the theoretical circuit modelling article, which increases the general understanding of the operation of the antennas, is placed before the other, more specific articles.

This summary combines the main results and places them within a larger scientific context. The summary is organised as follows: small-antenna fundamentals, matching and bandwidth enhancement methods, as well as traditional mobile terminal antennas are discussed in Chapter 2. Chapter 3 introduces compact coupling-based antenna structures, their implementation and design applications in free space. Chapter 4 handles the user-interaction issues. Chapter 5 includes the summary of the articles and Chapter 6 contains the final conclusions of the work.

2. Fundamentals of small mobile terminal antennas

2.1. Background theories and terms

2.1.1. Small antenna as a resonator

An antenna can be defined as "small" in different ways. In this thesis, small antennas are understood as electrically small antennas, which means that they can be enclosed inside a sphere of radius $a = \lambda_0/2\pi$, where λ_0 is the free space wavelength at the operating frequency [3]. Electrically small antennas store much more energy in the reactive near fields than is radiated into the far field in a time period. The outer boundary of the reactive near fields of small antennas is often considered to extend to a distance of $\lambda_0/2\pi$ from the surface of the antenna. The reactive near fields consist of the inductive and capacitive parts and the energy oscillates between the magnetic and electric fields. The resonance is achieved when the inductive and capacitive energy levels are equal and they cancel each other out. Since the operation of small antennas is based on the resonance phenomenon, it is advantageous to use the resonator theory in describing the operation of small antennas.

The quality factor Q describes the ratio between the energy W stored and the energy P dissipated per time period in the resonator. The general definition of the quality factor is [4]

$$Q = \omega_r \cdot \frac{\text{average energy stored}}{\text{energy loss per second}} = \frac{2\pi f_r W}{P}, \qquad (2.1)$$

where ω_r is the (angular) resonant frequency of a matched antenna. The quality factor of a small unmatched antenna can also be determined from the fundamental input impedance of the antenna using the following approximate formula [5]

$$Q = \frac{\omega_r}{2R(\omega_r)} \sqrt{[R'(\omega_r)]^2 + \left[X'(\omega_r) + \frac{|X(\omega_r)|}{\omega_r} \right]^2}, \qquad (2.2)$$

where $R(\omega_r)$ and $X(\omega_r)$ are the input resistance and reactance of the antenna, respectively, and $R'(\omega_r)$ and $X'(\omega_r)$ are their frequency derivatives.

The unloaded quality factor Q_0 describes all the losses P_0 in the resonator without the external feeding circuit. The losses include the resistive losses in the metallic and dielectric structures as well as the radiation "losses". Actually, (2.2) gives the unloaded quality factor since the input impedance takes into account all the losses of the antenna structure. In order to

achieve useful information, different loss mechanisms can be described with separate quality factors. The radiation quality factor Q_{rad} includes only radiation losses. Losses in the dielectric and conductor materials are described by dielectric and conductor quality factors Q_d and Q_c. By adding up the different loss powers, the connection between the different quality factors becomes [4]

$$\frac{1}{Q_0} = \frac{1}{Q_{rad}} + \frac{1}{Q_d} + \frac{1}{Q_c}. \tag{2.3}$$

There is a theoretical fundamental lower bound on the minimum radiation quality factor of a small antenna. If an antenna is enclosed inside a sphere with the radius a and it stores no energy inside the sphere, the smallest possible radiation quality factor of a linearly polarised antenna radiating at the lowest TE or TM resonance mode can be calculated from [6], [7], [8]

$$Q_{rad,min} = \frac{1}{k_0 a} + \frac{1}{(k_0 a)^3}, \tag{2.4}$$

where the wave number $k_o = 2\pi/\lambda_o$. This lower bound is typically called as the "Chu limit", and it is an important tool when estimating the maximum available bandwidth of an antenna of a particular size. However, due to the above-described ideal assumptions, especially that the energy stored inside the sphere is not taken into account, it is not possible to reach $Q_{rad,min}$ with any practical antenna.

A small antenna accepts the largest amount of power at the resonant frequency. Outside the resonant frequency the impedance of a small antenna changes rapidly and thus the impedance becomes the main factor, which limits the usable bandwidth. The impedance bandwidth is usually defined in terms of the return loss, L_{retn}, or the voltage standing wave ratio, *VSWR*. Near the resonant frequency, the impedance of a small antenna can be modelled as a series or parallel RLC equivalent circuit. The relative impedance bandwidth of the equivalent circuit can be derived and it can be calculated from

$$B_r = \frac{1}{Q_0}\sqrt{\frac{(TS-1)(S-T)}{S}}, \tag{2.5}$$

where S is the maximum accepted voltage standing wave ratio at the edges of the impedance band and T is the coupling coefficient [9]. With the optimal over coupling, $T = ½\cdot(S + 1/S)$, the theoretical maximum relative bandwidth becomes

$$B_{r,\mathrm{sr,max}} = \frac{S^2 - 1}{2SQ_0}. \tag{2.6}$$

In the discussion above, a small antenna is expected to be single-resonant. However, small antennas can also have multi-resonant operation which is a very efficient method to enhance the impedance bandwidth. That will be discussed later in Section 2.2.

2.1.2. Efficiency, directivity, gain

The radiation efficiency is defined as the ratio of the power radiated P_{rad} and the power P_0 accepted by the antenna [10]

$$\eta_{\mathrm{rad}} = \frac{P_{\mathrm{rad}}}{P_0} = \frac{Q_0}{Q_{\mathrm{rad}}} = \frac{R_{\mathrm{rad}}}{R_{\mathrm{rad}} + R_{\mathrm{loss}}}, \tag{2.7}$$

where R_{rad} and R_{loss} are the radiation and resistive loss resistances of an RLC resonator circuit that models the antenna at a certain (typically narrow) frequency band. The matching efficiency is defined as the ratio between the power P_0 accepted and the power P_{in} available at the antenna input [10]

$$\eta_{\mathrm{m}} = \frac{P_0}{P_{\mathrm{in}}} = 1 - |\rho|^2, \tag{2.8}$$

where ρ is the voltage reflection coefficient, which can be calculated either from [11]

$$\rho = \frac{Z_{\mathrm{in}} - Z_0^*}{Z_{\mathrm{in}} + Z_0}, \tag{2.9}$$

where Z_{in} is the input impedance of the antenna and Z_0^* is the complex conjugate of the impedance Z_0 of the feed, or from

$$|\rho| = \frac{VSWR - 1}{VSWR + 1}. \tag{2.10}$$

For example, if the return loss is 6.0 dB ($VSWR \approx 3$) at the edges of the impedance band, the corresponding reflection coefficient is about $|\rho| = 0.50$ and the matching efficiency at the edges of the impedance band is 0.75 = -1.3 dB. Total efficiency η_{tot} is the product of the radiation and matching efficiencies [10]

$$\eta_{\mathrm{tot}} = \frac{P_{\mathrm{rad}}}{P_{\mathrm{in}}} = \eta_{\mathrm{rad}} \cdot \eta_{\mathrm{m}}. \tag{2.11}$$

The directivity describes the directional radiation properties of an antenna. The directivity D to the direction of the maximum radiated/received power

is defined as the ratio between the maximum and average power densities [10]

$$D = \frac{S_{\max}}{\frac{1}{4\pi}\oint_{4\pi} S(\theta,\varphi)d\Omega}, \tag{2.12}$$

where $S_{\max}$ is the maximum power density [W/m²] in the far field region, $S(\theta, \varphi)$ is the power density function of an antenna, θ, and φ are variables in the standard spherical coordinate system. For electrically small antennas the directivity is close to 2 dBi [12].

Compared to the directivity, the gain takes into account the resistive losses in the antenna structure. The (electromagnetic) gain G is defined as [10]

$$G = \eta_{\text{rad}} \cdot D\,. \tag{2.13}$$

Furthermore, if the mismatching losses are also included, the realised gain G_{real} is used and it is defined as [10]

$$G_{real} = \eta_{\text{tot}} \cdot D\,. \tag{2.14}$$

Finally, the principal difference between the directivity, gain and realised gain is illustrated in Fig. 1. The effect of the impedance behaviour of a small antenna can be noticed in the realised gain curve.

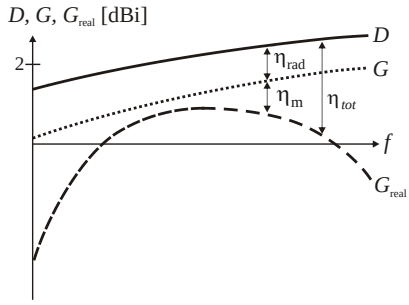

Fig. 1. Conceptual graph on the principal difference between directivity D, (electromagnetic) gain G and realised gain G_{real}.

2.1.3. Matching methods

In order to guarantee sufficient power transmission between an antenna and its feeding circuit, the antenna needs to be in resonance, i.e., the impedances need to be matched. The perfect matching (ρ = 0) is achieved when the impedances are each other's complex conjugates, see (2.9). However, the perfect matching can be achieved only at single frequency points (the theory will be introduced in Section 2.2.1), and thus a certain mismatching loss has always to be accepted across the defined (finite) operational band (2.8).

Antennas are either self-resonant or the resonance is produced with an external matching circuitry. Typical self-resonant antennas are open half-wave resonators (such as dipole and half-wave microstrip patch antennas) and quarter-wave resonators on a ground plane (such as monopole, helix, and planar inverted-F antennas). If the antenna is not in the resonance at the desired frequency band, or the resonance needs to be frequency tuned, a matching circuitry can be used.

State-of-the-art high-Q (low-loss) lumped elements (such as capacitors and inductors) are applicable in matching circuits roughly up to 2 GHz. Depending on the lumped components, they can also be used at frequencies higher than 2 GHz if the physical size of the component is clearly smaller than the wavelength – i.e., the largest dimension is smaller than, for instance, $\lambda/30$ [4], and the losses and parasitic effects are small enough. Basic lumped-element matching circuits consist of L-section networks, whose topology (eight possibilities) is defined by the location of the antenna impedance on the Smith chart [4], [13]. The designer can basically choose from two or four suitable matching circuit topologies. However, some topologies can provide a broader impedance bandwidth than others [13]. The design of L-section matching circuits is rather straightforward since closed-form design formulas are available, see [4], [13]. The matching circuitry can be implemented using distributed elements such as tuning stubs, or different kinds of transformers as well [4], [13]. However, the distributed elements cannot typically be used below 1 GHz, since the physical size of the matching circuitry would become too large to be placed inside a mobile terminal. Generally, the selection of the matching circuit technology is dictated by the losses, tolerances, available component values, printed circuit board area, and costs of the final implementation.

2.1.4. Specific absorption rate and hearing-aid compatibility

The specific absorption rate (SAR) is used as a measure to determine the time rate of the radio frequency energy absorbed per unit mass of human tissue. It is defined as

$$SAR = \sigma_{\text{eff}} \frac{|E_{\text{rms}}|^2}{\rho_{\text{d}}}, \tag{2.15}$$

where σ_{eff} is the effective conductivity of the tissue (defined with equation $\varepsilon_r = \varepsilon_r' - j\cdot\varepsilon_r'' = \varepsilon_r' - j\cdot\sigma_{\text{eff}}/\omega\cdot\varepsilon_0$), E_{rms} is the root-mean-square value of the electric field strength and ρ_{d} is the mass density. The SAR regulations are set to limit the RF exposure of the user of an RF device. The most important limit is for the spatial peak SAR in body (except in hands, wrists, feet and ankles)

and it is 2 W/kg (averaging mass 10 g) by ICNIRP [14] and 1.6 W/kg (averaging mass 1 g) by IEEE [15].

The hearing-aid compatibility (HAC) standard is set to avoid the electromagnetic compatibility problems caused by a mobile terminal on the operation of the hearing aid of the user, especially due to the near fields of the antennas [16]. The HAC standard limits the free space electric and magnetic field strengths around the earpiece of the terminal.

2.2. Bandwidth enhancement methods

The inherently narrow bandwidth of small antennas could, in principle, be enhanced by increasing the volume of the antenna, see (2.4). Typically, that is not feasible in modern mobile phones in which the volume reserved for the antennas is limited. If the volume is kept the same but the total efficiency is decreased, the bandwidth increases, see (2.5). In transmission the valuable battery power is then wasted in the losses, which is contrary to the desired long operation time, and in reception the signal-to-noise ratio degrades. Thus, the three important characteristics (bandwidth, efficiency and volume) of a small antenna are interrelated – i.e., one of these characteristics can only be improved at the expense of the other. Hence, the main challenge in small-antenna design is to find a reasonable case-specific trade-off between the three main properties. In addition, there are certain methods that might provide increased bandwidth resulting in more overall benefits than disadvantages. Those methods are 1) multi-resonant matching circuits, 2) frequency-tuneable matching circuits and 3) sacrificing efficiency, and they are presented in the following sections.

2.2.1. Multi-resonant matching circuits

So far, small antennas have been discussed as single-resonant resonators. It is a well known fact that the impedance bandwidth can be increased very efficiently with multiple resonances, which can be implemented with coupled high-Q (low-loss) resonators, for example, in the matching circuit [17]. The theoretical maximum bandwidth with one additional resonator (dual-resonant operation) can be calculated from [18]

$$B_{\mathrm{r,dr,max}} = \frac{\sqrt{S^2 - 1}}{Q_0}, \tag{2.16}$$

where S is the maximum allowed voltage standing wave ratio at the edges of the impedance band. Compared to the single-resonant case (2.6) the enhancement of the relative bandwidth is about 100%, which means doubled bandwidth [18]. With two and three additional resonators the

enhancement compared to the single-resonant case is about 150% and 180%, respectively [18]. With four or more resonators, the additional benefit gained by each resonator saturates fast towards the theoretical maximum bandwidth given by the Bode-Fano criterion [19], [20]:

$$B_{\mathrm{r,max}} = \frac{\pi}{Q_0 \ln\left(\frac{S+1}{S-1}\right)}. \tag{2.17}$$

The theoretical maximum bandwidth $B_{\mathrm{r,max}}$ is achieved with an infinite number of additional ideal resonators, and it is hence impossible to reach. Also in practice the number of additional resonators is limited due to the losses and complexity of the matching circuit. In addition, it can easily be seen from (2.17) that the perfect matching (S = 1) can be achieved only at single frequency points since the relative bandwidth $B_{\mathrm{r,max}}$ tends to null when S approaches 1.

Even though the theory for general multi-resonant matching circuits is well-known [11], [18], [19], [20], there does not exist general closed-form design formulas for such circuits. Only in some cases, when the input impedance is modelled with an equivalent circuit, such formulas have been derived. For example, for an antenna that can be modelled as a series RLC equivalent circuit over a certain bandwidth, a dual-resonant matching circuit can be designed using the analytical design formulas [21], [22]. In a general case the suitable topology of the matching circuit needs to be chosen depending on the input impedance of the antenna and numerous practical causes (such as available components, tolerances, losses, PCB area). Dual- and triple-resonant matching circuits will be applied in Chapters 3 and 4.

2.2.2. Frequency-tuneable matching circuits

One solution to implement a virtually enlarged overall bandwidth is to split the operation band into two or more non-simultaneously used sub-bands with an adaptive matching circuit. The typical ways to implement the adaptive matching are to use either 1) electrically adjustable tuning components (e.g., varactors) [23]-[25] or 2) parallel matching circuits for each sub-band separated by an RF switch [26]-[30]. The basic challenges of the frequency-tuneable matching circuits are the non-linearity and losses caused by the semiconductor tuning components [30], [31], [**III**]. In addition, the tuning circuit needs a control voltage and increases the complexity of the whole antenna system. Frequency-tuneable matching circuits will be further handled in Section 3.3.4.

2.2.3. Sacrificing efficiency

As was discussed earlier and can be seen from (2.5), an inherently narrow-band antenna can be designed in such a way that the impedance bandwidth is significantly increased at the expense of the overall total efficiency. Even though this method is not commonly recommended, in some specific cases, for instance, in mobile terminal antennas the total efficiency may have to be sacrificed in order to optimise other important characteristics such as the size of the antenna. There are basically three options:

1) One can use resistive loading of an antenna (lowering radiation efficiency artificially, for instance, with resistors in the input of the antenna or other lossy materials),
2) one can use resistive matching (attenuators), or
3) one can just accept higher mismatching between an antenna and its feeding circuit (lowering matching efficiency).

Comparing these three cases, it can be shown with the help of (2.6) and (2.16) that the third option provides the widest bandwidth for a given decrease of the total efficiency. For example, moderate mismatching is allowed in current mobile phones: Instead of the 10 dB return loss matching criterion, 6 dB is typically used in the cellular/transceiver systems, see for example, [18], [32]. When accepting a return loss of 6 dB instead of 10 dB, the theoretical increase of the bandwidth of an optimally overcoupled single-resonant antenna is as much as 78% (2.6). The price paid is about 0.74 dB lower total efficiency at the edges of the impedance band (2.8) and (2.11). On the other hand, if the total efficiency of the same antenna was decreased the same 0.74 dB by artificially decreasing the radiation efficiency, the increase of the optimally-coupled 10-dB return loss bandwidth would be only about 19% (2.6), (2.7), (2.8), (2.11). In the corresponding dual-resonant case (2.16), the improvement of the bandwidth is 63% when accepting mismatching and 19% when artificially decreasing the radiation efficiency. The lowest acceptable matching level needs to be considered separately in each case since there are typically also practical limitations, such as possible oscillations in the amplifier and distortion of the signal. However, in mobile terminals the transceivers are typically rather “robust” since, for example, the user’s hand fully covering the antenna may dramatically change its input impedance (as will be noticed in Section 4.1) and can therefore cause severe mismatching, which has to be tolerated.

2.3. Mobile terminal antennas

2.3.1. General requirements and trends

The important basic characteristics of mobile terminal antennas are the size, impedance bandwidth and total efficiency as described earlier. The following listing describes the general requirements of the antennas in more detail.

1) *Size and shape*: Generally the volume and thickness should be as small as possible whilst the performance requirements are met. The shape has to fit within the given platform, and also together with the other antennas and components such as the display, battery, camera, connectors, and acoustic devices.

2) *Matching*: The input impedance of the antenna needs to be well enough matched to the complex feed impedance which also changes as a function of frequency across the band of operation. Acceptable matching should be maintained also in the close vicinity of the user's head and hand. The cellular antennas operate in several radio systems and thus need to have multi-band operation.

3) *Efficiency*: Generally the efficiency should be as high as possible in order to guarantee reliable operation of the radio system and long operation time. In practice, relatively large losses introduced by the mismatching, lossy parts of the terminal, and the additional losses caused by the user have to be tolerated.

4) *Interoperability*: The isolation between the antennas should be good enough since otherwise signals leaking from a transmitter antenna to another antenna can block the operation of the respective system, and in addition the efficiencies of the antennas decrease.

5) *Directional pattern and polarisation*: An omnidirectional directional pattern in the azimuth plane is desirable (except in the direction of the user) due to the random orientation of the terminal and the incident wave(s). Due to the inherently low directivity of small antennas, the antenna designer cannot typically affect the directional pattern and polarisation, especially in the 1-GHz frequency range. However, the polarisation of the antenna is not obviously very important because typically in a complex multipath propagation environment some component of the incident waves has the same polarisation as the antenna.

6) *User-related regulations*: The antennas (or actually the whole terminal) must respect the specific absorption rate (SAR) regulations [14], [15] that are used to limit the radio frequency energy absorption per mass unit of the human tissue, see Section 2.1.4. Thus, the SAR values are a very important characteristic of the antennas. In addition, low SAR values are also desirable since typically less power is absorbed by the user and thus the radiation efficiency is higher [33]. The hearing-aid compatibility (HAC) standard, see Section 2.1.4, is regulated in the USA [16], but it might become widely introduced around the world. The performance of the terminal antennas in the user's hand grip is aimed to be regulated [34]. The standardised over-the-air (OTA) measurements are to be performed with homogeneous standard hand phantoms, introduced, for instance, by SPEAG [35] or IndexSAR [36].

7) *Commercial aspects:* In commercial mass production the manufacturability and testing should be cost-effective and reliable.

2.3.2 Short review of traditional internal antennas and future perspective

In current mobile terminals, the most commonly employed internal antennas are based on microstrip technology [32]. They have several advantages, such as planar structure, internal "built-in" structure, light weight, durability, low-cost, and easiness of manufacturing. The main disadvantage is the high radiation quality factor – i.e., inherently narrow impedance bandwidth. On the other hand, interfering out-band signals and noise are also attenuated effectively. The simplest microstrip antenna structure is a rectangular half-wave microstrip patch placed at a certain height above a ground plane [37]. The size of a microstrip patch antenna can be decreased significantly by short-circuiting one edge or corner of the patch. A planar inverted-F antenna (PIFA) is the most commonly used short-circuited planar antenna in mobile terminals [38]. Its physical length is typically slightly less than a quarter of the wavelength. One single PIFA element can be designed to perform, for example, penta-band operation for GSM850, E-GSM, GSM1800, GSM1900 and 3G, by shaping the element and utilising multi-resonant techniques (such as parasitic elements). The design of such PIFAs is presented in text books, see for instance [32], [39]. A variant antenna of the PIFA is an inverted-F antenna (IFA) which consists of a short-circuited quarter-wavelength-long wire or strip. An ILA is an inverted-L antenna, which is a variant of a monopole on a ground plane. IFAs and ILAs are useful antennas, for example, for GPS, WLAN and

Bluetooth [32], [40]. Fig. 2 shows a separate PIFA-IFA antenna unit, which is positioned in the end of a mobile terminal.

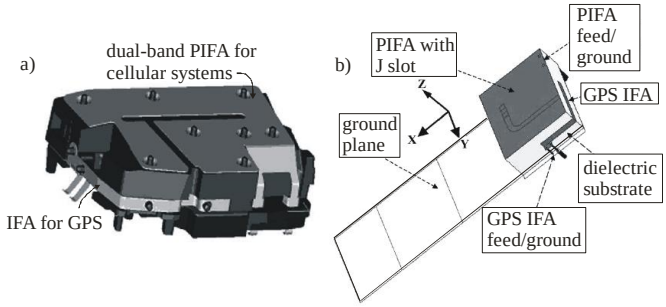

Fig. 2. a) PIFA-IFA antenna unit for mobile terminals [32], and b) placing of the antenna unit in the end of the ground plane of the printed circuit board of the terminal [40].

However, the traditional self-resonant antenna solutions, as introduced above, might not be viable to provide broadband and/or multi-band operation with sufficiently thin and small antenna structures for future multi-function terminals, such as LTE, 4G and cognitive radios. Thus, novel antenna solutions are required. One option is to exploit all the available conductive parts of the terminals as radiators. It is already well known that the metallic ground plane and other "large" electrically conductive parts of a mobile terminal play a significant role in the radiation of the traditional self-resonant UHF-band antennas. This phenomenon can be further exploited to optimise especially the *impedance bandwidth-to-volume* ratio of the UHF-band antennas [41]. That topic will be studied in greater detail in the next chapter.

2.3.3 Design strategies and available solutions for UHF-band digital television receiver antennas in mobile terminals

In addition to the radio systems mentioned in the previous sections, today's multisystem radios may also include a digital television (DTV) receiver, which is used as an application example of the lower UHF band – i.e., below 1 GHz – broadband receiving antennas studied in this thesis. A systematic study of the implementation, design and analysis of such antennas in mobile terminals covers a remarkable part of the articles of this thesis [**II**], [**IV**] and [**VII**]. The antenna design strategies, performance parameters and existing antenna solutions for the DTV in mobile terminals are handled comprehensively in [**II**] and discussed also in this section. New antenna solutions will be handled in Section 3.3.3 and the user effect issues in Section 4.3.

DVB-H (Digital Video Broadcasting-Handheld) is used as a digital television (DTV) standard in this thesis since it is a typical broadband DTV standard for mobile terminals and used at least in Europe [42], [43]. However, there are also other broadcasting digital television standards for handheld devices, such as ATSC-M/H (Advanced Television Systems Committee - Mobile/Handheld) in North America, ISDB (Integrated Services Digital Broadcasting) "1seg" in Japan and South America, and DTMB (Digital Terrestrial Multimedia Broadcast) in the People's Republic of China. All of them operate in the lower UHF band, and thus the design methods presented in this thesis can be applied to other standards, too.

The frequency band of DVB-H is 0.47 - 0.75 GHz (B_r = 46%) in mobile terminals, which supports also an E-GSM system at 0.88 - 0.96 GHz. The respective wavelength for the DTV system is 400-640 mm. As the typical handset length is 100-130 mm, an internal DTV antenna is electrically rather small. Due to the inherent physical limitations described in Section 2.1, the implementation of small broadband DTV antennas is very challenging across the DTV band with the typical matching criterion (6 dB return loss) of current cellular antennas. Thus, the designer has to use all possible means to maximise the impedance bandwidth of the antenna. Basically, the design consists of three aspects:

1) minimising the radiation quality factor of the antenna structure,
2) sacrificing the total efficiency to the lowest acceptable level (Section 2.2.3),
3) using optimal matching methods including tuneable matching circuit and/or multi-resonant broadband matching (Sections 2.2.1 and 2.2.2).

What comes to Item 1), "traditional" terminal antennas (see the previous section), such as PIFAs and IFAs, could be utilised as DTV antennas but the impedance bandwidth would be too narrow or the antenna size would become too large to be placed inside a handset [44], [45]. The new antenna solutions based on the exploitation of the radiation of the ground plane will be handled in the next chapter.

Concerning Item 2), a basic requirement for radio systems is to reach a sufficient signal-to-noise ratio over the frequency band of operation. In order to minimise the size of the antenna element, the design principle of the DTV antennas is to provide performance (efficiency) which is just enough for guaranteeing the operation with a certain reliability level [46], [**II**]. It is hence possible to sacrifice the efficiency since the DTV is a receive-only system and typically a lower total efficiency compared to a transceiver

can be accepted in receiving antennas [47]. Based on the rough estimation performed in [**II**], the lowest acceptable total efficiency for a DTV antenna is in the order of -16 to -12 dB over the band. Similar calculations have been performed also in [46].

The expected DTV antenna performance in the DVB-H standard followed in this paper has been given in terms of the realised gain (2.14) [42], [43] which consists of the directivity (2.12) and the total efficiency (2.11), see Fig. 1. In the DVB-H system specifications, the realised gain of the antenna placed inside a real mobile terminal is expected to be in the order of -10 dBi at 0.47 GHz and to increase linearly in decibels to about -6.5 dBi at 0.75 GHz. When the directivity (2 dBi for electrically small antennas [12]) is excluded, the total efficiency across the band is expected to be in the order of -12 to -8.5 dB according to the above-mentioned realised gain limit. Concluding the calculations above, the expected performance of a DTV antenna is at least 3.5 dB higher than the estimated lowest acceptable total efficiency. In this thesis, the presented realised gain limit is considered as the performance specification for internal DTV antennas. The means how to sacrifice the efficiency are discussed in Section 2.2.3 and will be used in practice in Section 3.3.3.

What comes to Item 3), due to the inherently narrow impedance bandwidth of small antennas, tuneable matching seems like a reasonable choice for DTV antennas. However, one challenge is the non-linearity caused by the semiconductor tuning component, which becomes a problem especially during the simultaneous use of E-GSM transmission if a part of the transmitted strong E-GSM signal is coupled to the DTV antenna. In addition, the tuning circuit is typically lossy, and it needs a control voltage and increases the overall complexity of the whole system. On the other hand, the high linearity and fixed matching of passive implementation of the antenna motivates the use of broadband multi-resonant antennas whenever a suitable small antenna can provide sufficient performance. In the end, the matching strategy (tuneable, broadband or their suitable combination) is dictated by the available volume for the antenna, available electrical components (including antenna technology), and the required performance of the system.

The available internal DTV antenna solutions are divided into two main categories according to the matching method (Item 3). The first group is formed by the electrically tuneable antennas which create an instantaneous resonance at a suitable frequency so that at least a single 8-MHz channel is covered. Examples of the electrically-tuneable antennas are introduced in [23], [24], [48], [49]. The second main group is formed by antennas with

fixed broadband (typically multi-resonant) matching. As stated above, the main challenge is to cover the whole DTV band with a sufficiently small antenna having the required realised-gain performance [50]-[55].

3 Compact coupling-based mobile terminal antennas

3.1 General

The ground planes of the printed circuit board (PCB), EMC shielding and other electrically conductive parts (like display and its frame) of a handheld device create a solid RF ground plane, called a *chassis*. This electrically conductive chassis has a significant effect on the impedance and radiation properties of the antennas. Actually, the required impedance bandwidths of the internal antennas would not be possible without the presence of the chassis at the lower UHF frequencies (below 1 GHz), because the representative antenna element is alone electrically too small to be able to cover the bandwidths required, for example, for DTV and GSM850/E-GSM (see Section 2.1.1). This chapter describes and studies how the chassis can be exploited as a part of the antenna structure for the future's systems in the UHF band.

Traditional mobile terminal antennas, such as a planar inverted-F antenna (PIFA), create the antenna resonance and couple radiative common mode currents at the edges of the chassis. A large part of the antenna element volume is "wasted" for creating the resonance [56]. Since the antenna element itself is not a significant radiator below 1 GHz, the volume occupied by the element can be decreased significantly by introducing *non-resonant compact coupling-based antenna* structures, whose principal function is to only couple radiative common mode currents at the edges of the chassis, [56], [57]. That is the reason why they are called compact *coupling*-based antennas. Since the coupling structure itself is non-resonant, the resonance of the antenna is created with a separate matching circuitry outside the coupling structure, see Section 2.1.3. The available impedance bandwidth typically stays at least the same although the antenna element can be made significantly smaller than, for instance, a PIFA. Therefore, in order to achieve the minimum volume of the coupling structure whilst providing sufficient bandwidth, one needs to exploit the chassis radiation by maximising the coupling to the chassis wavemode(s) [57].

Different coupling structures can be categorised according to the way the coupling is done. The radiative common mode currents on the edges of the chassis can be created via electric or magnetic fields and/or using galvanic coupling, which all are well-known electromagnetic near-field phenomena. The coupling mainly via electric fields can be implemented with a *capacitive coupling element* [56], [57]. A galvanic feed can be created using

a *direct feed* across an impedance discontinuity, such as a slot, [53], [58], [**IV**]. An *inductive coupling loop* couples via magnetic fields [59]. In this thesis, capacitive coupling elements and direct feed antenna structures are to be studied, and inductive coupling loops are left for a future research topic.

Non-resonant compact coupling-based structures have many possible advantages compared to traditional self-resonant mobile terminal antennas, such as PIFAs [57], [**II**]. One single element can be optimised to couple relatively strongly to the radiative chassis currents in a wide frequency band and thus the antenna can be matched at any selected frequency band with a suitable external matching circuitry. In principle, any available floating metallic pieces, for example, in the cover of the terminal, might be used as a "coupler". In addition, multi-resonant operation and electrical frequency tuning can also be implemented rather easily in the matching circuitry, see Sections 2.2.1 and 2.2.2. Thus, it is possible that future's mobile terminals have only a few antenna elements instead of several elements used in today's terminals. That is the reason why such non-resonant coupling-based antennas are studied in this thesis.

3.2 Effect of the terminal chassis on the operation of the antenna

As is well known, the terminal chassis supports flat-dipole-type common mode current distributions and has certain resonant wavemodes. The characteristic mode theory provides a useful tool to study the radiation characteristics of the wavemodes of a plain chassis [60], [61]. It is possible to numerically calculate the resonant frequencies and the respective quality factors. In [62] the method was applied to analyse 100 mm × 40 mm solid thin mobile terminal chassis. The first four resonant frequencies of the wavemodes are at 1.26, 2.68, 2.74, and 3.08 GHz and the respective Q values are 2.3, 3.0, 2.5 and 2.3. The first two modes represent the major axis (long edge) half- and full-wave dipole modes. The third mode at 2.74 GHz is the minor axis (short edge) half-wave mode and the fourth mode at 3.08 GHz is the magnetic dipole mode. Especially, the major axis low-Q half-wave dipole mode plays an essential role as a radiator at lower UHF frequencies as it contributes at a broad band around the resonant frequency. In practice, the current distribution of the chassis at a given frequency is the superposition of these wavemodes. At certain frequencies between two wavemodes, for instance, major axis half- and full-wave modes, the currents of the wavemodes might be opposite in phase and they partly cancel each other. Thus, the chassis has an anti-resonance, in which

the Q value has a local maximum. An example will be shown in the next section.

For different-sized chassis the resonant frequencies are scaled inversely proportionally to the length. Approximate formulas for the major axis half- and full-wave resonant frequencies are given in [56]

$$f_{r,half-wave} \approx (0.73 \cdots 0.78) \cdot \frac{c}{2l}, \text{ and} \tag{3.1}$$

$$f_{r,full-wave} \approx (0.83 \cdots 0.85) \cdot \frac{c}{l}, \tag{3.2}$$

where c is the speed of light in free space and l is the physical length of the chassis. The electrical length of the chassis is longer than the physical length due to the open-end extension.

The characteristic mode analysis described above is based on applying a plane wave excitation on a plain chassis. However, an antenna like this does not exist alone. In mobile terminals a certain coupling structure is required to excite the radiative low-Q chassis wavemodes. A circuit-theoretical approach on the combined performance of a self-resonant mobile terminal antenna element and the chassis is presented in [56]. The separate wavemodes of the antenna element and the chassis are modelled with coupled resonators, which are further described by the respective resonant frequencies and Q values. It was shown that a traditional self-resonant antenna element like a PIFA contributes about 10% to the total radiated power at 0.9 GHz. The rest is radiated by the chassis wavemode(s). At 1.8 GHz the contribution of the antenna element is much larger, about 50%. Especially, it was shown that even though the antenna element, or generally the coupling structure, is made practically non-radiating (very high Q value), the radiation of the chassis low-Q wavemodes makes it anyway possible to achieve large impedance bandwidths whenever the excitation of the chassis wavemode(s) is strong enough.

Furthermore, the bandwidth maxima of antennas, which exploit the chassis as a radiator, are achieved at the resonant frequencies of the chassis wavemodes [63]. As the resonant frequency of the lowest order wavemode of the chassis (with dimensions 100 mm × 40 mm) is above 1 GHz (3.1), the resonant frequency of the chassis is thus not optimal from the bandwidth point of view, for instance, for the lower UHF-band digital television receiver (DVB-H). Therefore, one should also try, if possible, to tune the chassis resonant frequency to match the centre frequency of the intended radio system in order to maximise the bandwidth. The dimensions, especially the length, of the chassis affect also the specific absorption rate

(SAR) and the radiation efficiency. In [64] it has been shown that when the bandwidth reaches it maximum due to the resonance of the chassis wavemode, an increase in the head SAR and a decrease in radiation efficiency take place. Thus, the SAR values are significantly affected by the chassis wavemodes.

3.3 Antennas with capacitive coupling element

3.3.1 Basic concept and earlier antenna solutions

The coupling method affects significantly the excitation of the chassis wavemodes and thus the impedance and radiation characteristics of the whole antenna. Different numerical studies on the effect of the coupling methods have been presented. In [57] a non-resonant small feed probe (very high Q value), which couples mainly capacitively through the electric fields, was used as a "coupler". It was shown that in order to couple most strongly to the dominant chassis wavemode and thus achieve the lowest possible radiation quality factor, the capacitive coupler needs to be co-located with the electric field maximum of the respective wavemode. Therefore, it is important to understand the current distributions and the reactive near fields of the chassis wavemodes described in the previous section. For the major axis wavemodes the electric field maxima are located at the short edges of the chassis, especially near the corners. Furthermore, the coupling can be made stronger by placing the coupler beyond the short edge of the chassis. The coupler can be bent over the edge of the chassis so that the surface of the CCE is perpendicular to the electric fields of the dominant wavemodes of the chassis [57], [62], see Fig. 3a. The equipotential surfaces in Fig. 3b show the optimal shape of the coupler. In [65] the same observations were confirmed with a small rectangular patch antenna mounted on a chassis. In addition, the coupler also affects the resonant frequencies of the wavemodes by tuning them downwards in frequency [65]. Generally, the characteristic mode theory can also be used to study the combined performance of the coupler and the chassis and the optimal location of the coupler relative to the chassis [62], [65]-[67].

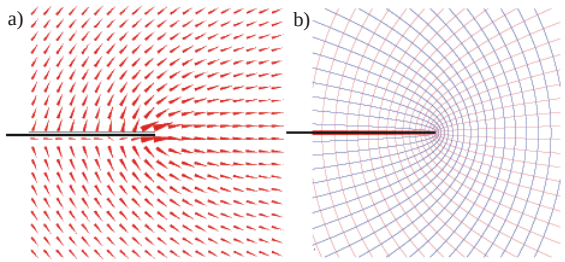

Fig. 3. a) Side view of the electric fields on the mid-point line of the short edge of a 100 mm × 40 mm plain chassis at the major-axis half-wave mode, and b) the corresponding equipotential surfaces. The picture is from [62].

The feasibility of such non-resonant capacitive coupling elements (CCE) for mobile terminal antennas was introduced in [56], and more comprehensively studied in [57]. Four prototypes, two at 0.9 GHz and two at 1.8 GHz, were designed, manufactured and measured. A comparison to reference PIFAs operating on the similar chassis at the same frequencies was performed. The results clearly showed that the size of the element is much smaller and the impedance bandwidth somewhat broader with CCEs than those with the reference PIFAs. The reason for the superior *bandwidth-to-element-volume ratio* of the CCE compared to the PIFA is that CCEs excite the dominant wavemode(s) of the chassis more strongly than the PIFAs. This happens obviously due to the fact that the PIFA does not couple optimally since the electric fields near the shorting pin are weak and thus the coupling is reduced [57]. The impedance bandwidth, specific absorption rate and radiation efficiency behaviour of CCE antennas at a wide frequency range were studied in the talk position with head and hand in [68], and in the vicinity of a large dielectric block in [69]. The results of [68] and [69] also suggest that the SAR and radiation efficiency of CCE antennas are strongly affected by the chassis wavemodes in the UHF band.

Fig. 4a shows an example of a basic CCE antenna structure (a fully high-conductivity metal structure) without the matching circuit which would be attached next to the CCE feed. In this thesis, the width of all CCEs is chosen to be equal to the width of the chassis since a narrower element would provide a smaller impedance bandwidth, especially at the lower UHF frequencies. On the other hand, the elements wider than the chassis would provide a larger bandwidth but they might be difficult to integrate into real terminals in practise. Differently shaped CCEs, such as the CCEs placed in the corners of the chassis, are also predefined outside the scope of this thesis. However, their operational principle is the same as in simple wide CCEs emphasised in this thesis.

The fundamental input impedance of the unmatched antenna of Fig. 4a was simulated with a method of moments-based electromagnetic simulator IE3D [70], and it is shown on the Smith chart against 50-ohms reference impedance in Fig. 4b. The unloaded quality factor calculated from the fundamental input impedance using (2.2) is shown in Fig. 4c. The effect of the major axis wavemodes at 1.17 and 2.61 GHz can clearly be seen both in the input impedance and the unloaded quality factor. Due to the minima of the unloaded quality factor at 1.17 and 2.61 GHz, the impedance bandwidth maxima of the matched antenna would be achieved at the same frequencies, see (2.5). Between the half- and full-wave modes (at about 1.9 GHz), the chassis has the anti-resonance since the common mode currents of the half-wave and full-wave modes partly cancel each other.

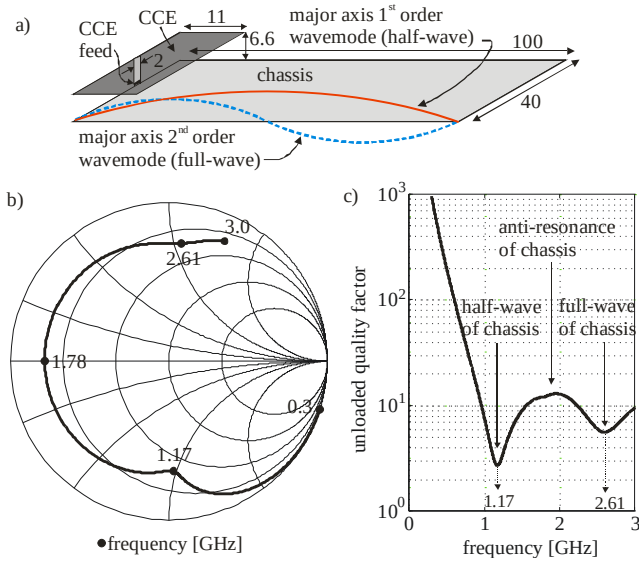

Fig. 4. a) Basic capacitive coupling element (CCE) mounted on a thin mobile terminal chassis (dimensions in mm), with principal common mode current distributions of the two lowest-order major axis wavemodes of the chassis, b) the fundamental input impedance against 50-ohms reference impedance, and c) the unloaded quality factor (2.2) of the CCE chassis antenna as a function of the frequency.

Fig. 5 shows the far-field directional pattern cuts of the CCE antenna of Fig. 4a in free space. The patterns are given as the directivity (2.12) and the radial unit is dBi. At 1.17 GHz (half-wave of chassis) and below it (e.g., at 0.50 GHz), the shapes of the patterns fully resemble that of a half-wave dipole antenna, “doughnut”. That is obvious since the common mode currents of the chassis are responsible for the main part of the radiation. The directivity to the direction of the main lobe is about 2 dBi which is also typical for dipole-type radiators. At 2.61 GHz (full-wave of chassis) the

shapes of the patterns resemble, to some extent, those of full-wave dipole antennas which feature two main lobes per hemisphere. However, due to the increased radiation of the CCE, the radiation is more directed to the upper hemisphere (maximum directivity about 5 dBi) than to the lower hemisphere (maximum directivity 2 dBi). At the anti-resonance of chassis (1.90 GHz), the directional pattern is some kind of combination of the patterns at 1.17 and 2.61 GHz.

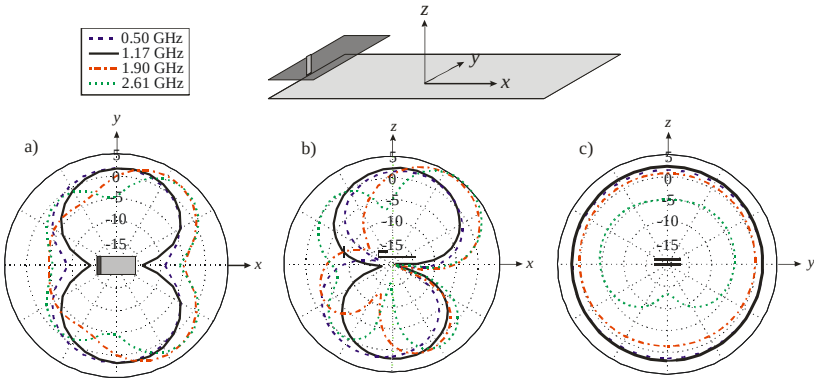

Fig. 5. Simulated far-field directional pattern cuts of the CCE antenna of Fig. 4a (directivity in dBi) in the a) azimuth plane (elevation angle 90°), b) elevation plane (azimuth angle 0°), and elevation plane (azimuth angle 90°).

The presented CCE concept suits also for multi-band and/or frequency-tuneable antennas by exploiting the modularity of the compact coupling structures [26], [71]. One single CCE can be used with a tuneable matching circuitry – the frequency tuning will be further handled in Section 3.3.4. An alternative option is to use separate CCEs (all including own matching circuits) for each frequency band [71]. A record-small quad-band antenna for GSM850/E-GSM/GSM1800/GSM1900 exploiting two separate CCEs with their feeds combined together into one single feed using a diplexer was proposed in [72].

3.3.2 Equivalent circuits

As was already discussed in Section 3.2, a circuit-theoretical approach on the operation of the combination of a self-resonant antenna and a mobile terminal chassis was presented in [56]. Furthermore, an equivalent circuit for a monopole antenna on a chassis was derived in [73]. Those two papers provide a general basis for a more-detailed circuit model proposed for single-CCE antennas in this thesis [**I**], see Fig. 6. All the three excited wavemodes of the CCE antenna (one from the CCE and two from the chassis, see also Fig. 4a) are modelled in the UHF band (0.3-3 GHz) which

makes the proposed model fairly broadband. The presented circuit model aims at an improved overall understanding of the operation of the CCE antennas: it gives a helpful physical explanation of the operation. In addition, it provides a useful circuit-theoretical tool for analysing the combined performance of the CCE and the terminal chassis, but it also helps in analysing how different parts of the structure contribute to the radiation and input impedance of the entire structure.

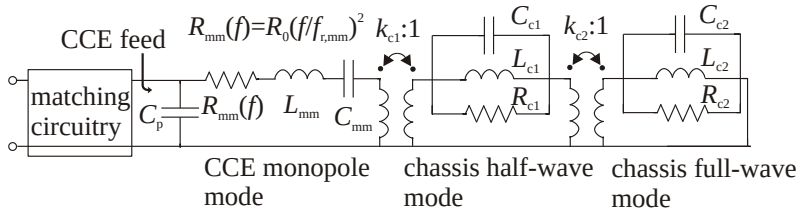

Fig. 6. Equivalent circuit for the CCE antennas in the free space.

Each of the excited wavemodes of the CCE and the chassis are modelled using an RLC resonator circuit, in which the resistors model the power "loss" by the radiation in the far field (and possible resistive losses in the antenna structure) and the reactive elements model the energy stored in the near fields. The combination of the wavemodes is modelled as a set of coupled resonators whose coupling to each other is modelled as an ideal transformer, an approach adopted from [56]. The parallel capacitor C_p in Fig. 6 is a parasitic component, which is required to satisfy the condition of zero impedance at infinite frequency for the CCE feed. The component values of the equivalent circuit are determined from the resonant frequencies and the respective unloaded quality factors of the wavemodes, and based on the comparison with the IE3D-simulated impedance of the antenna structure. All the component values, the resonant frequencies and quality factors of the resonators derived for the antenna Fig. 4a are shown in [**I**]. The principal impedance behaviour of the CCE antenna can be modelled with a good accuracy with the proposed circuit model, see Fig. 7a. Even though the circuit model and component values are derived for the particular structure shown in Fig. 4a, the same derivation procedure could be applied to other CCE structures with changed shape or dimensions, or additional excited wavemodes. The additional chassis wavemodes would be parallel RLC resonators placed in a cascade configuration, and the CCE wavemodes series RLC resonators in a shunt configuration. Further details of the antenna and the circuit model are explained in [**I**].

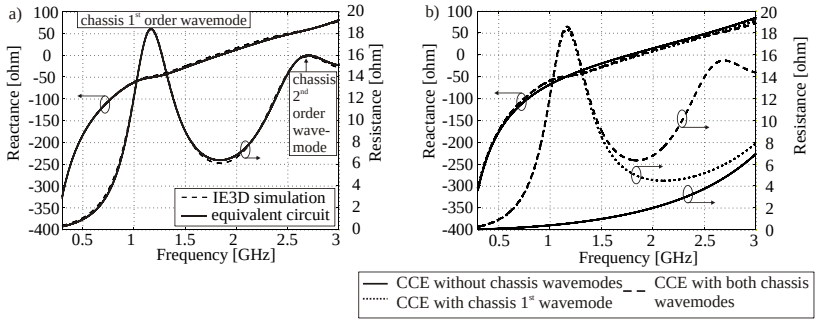

Fig. 7. a) Comparison between the impedances seen from the CCE feed of the circuit model in Fig. 5 and the IE3D simulated CCE structure shown in Fig. 4a. b) The effect of the chassis wavemodes on the impedance, the calculations performed by the circuit model.

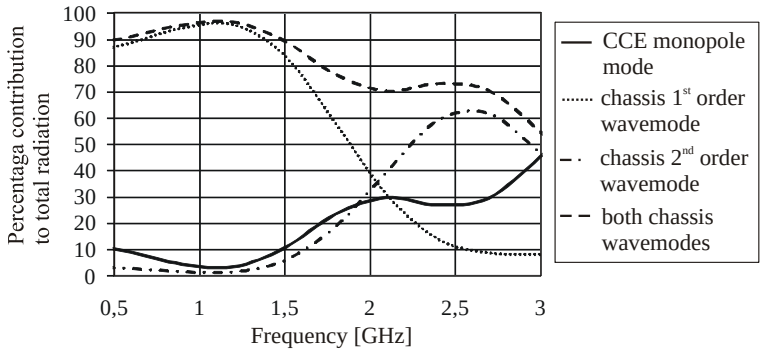

Fig. 8. Percentage contribution of each wavemode to the total radiation losses of the circuit model.

The proposed circuit model can be used to separate the effect of the CCE and chassis wavemodes on the impedance and radiation. The impedance calculated from the circuit model with and without the effect of the chassis wavemodes is shown in Fig. 7b. Firstly, the reactance behaviour is mainly determined by the CCE monopole mode. This is due to the fact that the Q value of the CCE is much higher than those of the chassis wavemodes. For the same reason, the resistance behaviour is mainly determined by the chassis wavemodes, especially in the lower UHF frequencies where the effective resistance of the CCE is very small. The contribution of each resonator to the radiation is also analysed. The percentage contribution of each wavemode to the total radiation "losses", calculated by the equivalent circuit, is shown in Fig. 8. It can be seen that the overall contribution of the chassis wavemodes to the radiation is very significant. At the 1-GHz frequency range as much as 95% is radiated by the chassis wavemodes, and at the 2-GHz range the chassis still contributes at least 70%. Both values are

consistent with the results derived from the surface current integrals in [57]. In Section 4.2, the above-presented equivalent circuit will be further applied to study the effect of lossy dielectric material (such as the user) on the operation of CCE-based antennas.

3.3.3 Implementation of broadband lower UHF-band receiving antenna – application example digital television receiver system

A remarkable part of this thesis handles the implementation, design and analysis of lower UHF-band broadband receiving antennas based on the CCE concept [**II**], [**VII**]. The digital television receiver (DTV) system is used as an application example, but the design methods could be used also for other broadband systems operating in the UHF band, such as low-band LTE or the spectrum sensing of the cognitive radio [2], [74].

The design strategies of the DTV antennas are discussed comprehensively in [**II**] and revised in Section 2.3.3. It was concluded that the total efficiency of the antenna can be decreased to a level which is just good enough to ensure a sufficient signal-to-noise ratio and in that way make the size of the antenna sufficiently small (Item 2 in Section 2.3.3). In addition, dual- and triple-resonant matching circuits will be applied in this thesis to achieve large enough impedance bandwidth (Item 3 in Section 2.3.3).

By strengthening the coupling between the CCE and chassis wavemode(s) (k_{c1}, k_{c2} in Fig. 6), a smaller radiation quality factor of the whole antenna can be achieved (Item 1 in Section 2.3.3). In order to maximise the coupling to the dominant chassis wavemode whilst minimising the overall size of the CCE, the CCE needs to be placed beyond the short edge of the chassis [57], [62]. In addition, the element should be bent over the shorter edge of the chassis so that the surface of the CCE is perpendicular to the electric fields of the dominant wavemodes of the chassis, see Fig. 3, Fig. 9a and compare also with Fig. 4a. The vertical part of the CCE could be further lengthened on the upper side of the chassis, see Fig. 9a, but that place is typically reserved for other components (such as connectors, buttons, microphone/earpiece, camera) in real terminals.

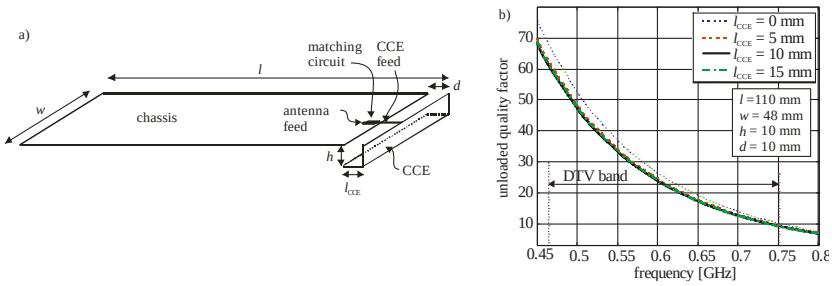

Fig. 9. a) CCE antenna structure used for digital television receiver, b) unloaded quality factor of the CCE antenna with the selected dimensions.

Next, the optimal shape of the CCE in Fig. 9a with the dimensions l = 110 mm, w = 48 mm, h = 10 mm, and d = 10 mm is studied. l_{CCE} is a variable, whose value is 0, 5, 10 and 15 mm. The input impedance of the antenna structure with different l_{CCE} is simulated with IE3D, and the respective unloaded quality factors based on (2.2) are shown in Fig. 9b. It can be seen that when $l_{CCE} = d$ (= 10 mm in this example), the smallest radiation quality factor and thus the largest impedance bandwidth can be achieved. The same result based on a similar antenna structure but with the dimension l = 135 mm, w = 75 mm, h = 4 mm, and d = 5 mm is presented in [28]. It seems that $l_{CCE} = d$ gives both the smallest radiation quality factor and minimises the volume of the CCE (l_{CCE} = 0 mm would not give any smaller CCE size since, in principle, the whole empty space between the CCE and the chassis needs to be reserved for the antenna). Thus, such CCEs are used in this thesis for DTV antennas. Further decrease in the radiation quality factor can be achieved by increasing the size of the CCE – i.e., increasing d and/or h. Generally, the optimal shape of CCE needs to be studied separately for each CCE and chassis combination at the frequency bands used.

A DTV antenna prototype in a tablet-size terminal was presented in [**II**]. The CCE structure was similar to Fig. 8a with the dimensions l = 135 mm, w = 75 mm, h = 4 mm, and $d = l_{CCE}$ = 5 mm, see Fig. 10a. Note that in this thesis the "tablet-size" terminal does not refer to today's "finger computers" whose size is about 250 mm x 200 mm [length x width]. The prototype fulfills the realised gain specification (see Section 2.3.3) with at least a 3.5-dB margin at 0.47-0.75 GHz in free space, see Fig. 10b. The matching across the DTV band is at least 2 dB in terms of return loss, see Fig. 11. The 2-dB return loss instead of the typical 6 dB is acceptable firstly due to the fact that the antenna is used in reception only, detailed reasons are stated in [**II**], see also Section 2.2.3. Secondly, the implementation losses introduced by the other parts of real terminals such as printed circuit board (typically FR4), plastic covers, display, battery, earpiece, and microphone, will cause additional losses (typically in the order of 3 dB [46], [75], [76]) and hence

improve the matching level. Thus, the above-presented 3.5-dB realised-gain performance margin to the specification is justifiable in the simplified antenna prototype, which has only losses from the low-loss PCB substrate (Rogers/Duroid [77]), metal structures and the matching circuit (Murata's chip coils and capacitors [78]). It can be concluded that it is relatively easy to implement a sufficiently small CCE having required realised gain performance in tablet-size terminals which enable also relatively large display and are thus fairly popular today. The far-field directional pattern, demonstrated also in [**VII**], is similar "doughnut" that was shown in Fig. 5 at 0.5 GHz.

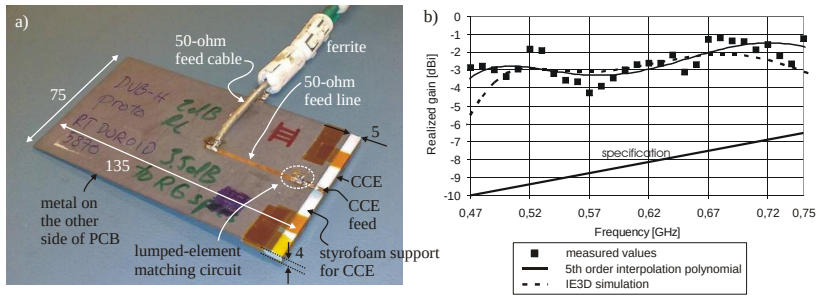

Fig. 10. a) Photograph of the tablet-size DTV antenna prototype, and b) simulated and measured realised gain of the prototype.

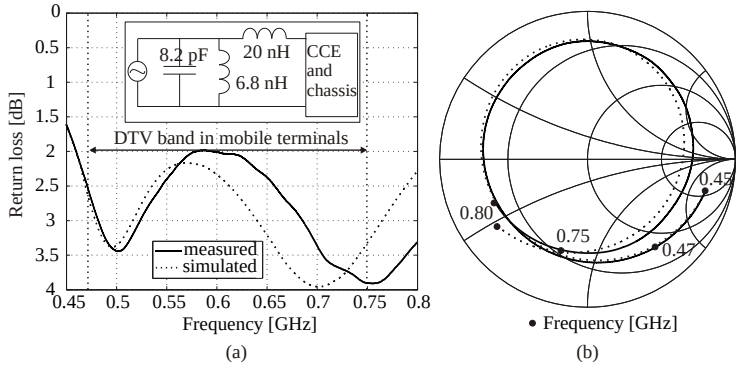

Fig. 11. Simulated and measured return loss of the tablet-size DTV prototype a) in the Cartesian coordinate system and b) on the Smith chart.

The implementation of DTV antennas in smaller-size terminals is possible as well. However, decreased dimensions, especially the length *l*, of the chassis increase the resonant frequency of the first-order wavemode of the chassis (3.1). Thus, the contribution of the chassis to the total radiation resistance at the given frequency band (0.47-0.75 GHz) decreases. That can be understood from Fig. 7ab. Hence, the decrease of the radiation resistance decreases the overall performance (efficiency/realised gain) of the antenna (2.7), (2.8), (2.9), (2.11), and (2.14). Thus, in order to maintain

the performance of the antenna, the decrease of the total radiation resistance needs to be compensated by further increasing the coupling (k_{c1} in Fig. 6) and/or by decreasing the radiation quality factor of the CCE monopole mode (basically R_{mm} increase in Fig. 6). Hence, the size of the CCE has to be increased – i.e., d and/or h of the CCE have to be increased, see Fig. 8a. The limits for the size of the CCE for different-size terminals were systematically studied in [**II**]. The study is performed with a lossless antenna structure and ideal matching circuit components since with realistic components the comparison of the CCE size between different-sized terminals would not be consistent and fair. The 3-dB margin to the realised gain specification was still reserved for compensating the implementation losses of a real terminal, as described earlier in this section. The EM-simulated results in [**II**] indicate that when exploiting optimal triple-resonant matching circuit (five components), relatively thick (h = 9-14 mm, see Fig. 9a) CCEs are required in today's typical-size (l = 110 mm, w = 48 mm, and $d = l_{CCE}$ = 5-10 mm) terminals. Thus, it is very challenging to meet the required realised gain including the 3-dB margin in typical-size terminals with thin and small CCEs. In order to make the CCE thinner (smaller h) without further increasing the distance d, the performance of the antenna has to be slightly sacrificed. For example, it was shown that in the above-discussed typical-sized terminal, 3 mm thinner CCE (from 9 mm to 6 mm) is possible with only 0.3 dB sacrifice of the realised gain margin.

In order to demonstrate the realistic operation of such DTV antennas, a simulated design including realistic (lossy) triple-resonant matching circuit components was presented in [**II**]. The dimensions of the design are l = 110 mm, w = 48 mm, h = 6 mm, and $d = l_{CCE}$ = 10 mm. The DTV antenna design has at least 2.8 dB return loss matching, at least 2.5 dB margin to the realised gain specification, and a minimum of 22 dB isolation to the CCE-based E-GSM antenna mounted on the same chassis. This design is considered to be a good compromise between the size of the CCE and the performance of the whole antenna. It was also noticed that the realised gain of the DTV antenna is slightly improved (about 0.5 dB) by the presence of the E-GSM antenna. That is due to the fact that the CCE of E-GSM lengthens the electrical length of the chassis (as explained in Section 3.3.1) and thus the half-wave resonant frequency is tuned to a lower frequency causing a slight increase in the radiation resistance of the DTV antenna (that can be understood based on Fig. 7a). Furthermore, the increased radiation resistance improves the total efficiency (2.7) and thus the realised gain (2.14).

The results of [**II**] also show that since the effective radiation resistance of CCE antennas is rather low at the frequencies below the first-order wavemode of the chassis (see Fig. 7a), the resistive losses (typically a few ohms of magnitude) in the matching circuit affect relatively much the radiation efficiency (2.7). Thus, it is very important that the losses of the matching circuit components are modelled realistically with the S parameters of real components from the very beginning of the real design process of CCE antennas.

Another issue that has to be taken into account is the interoperability between the antennas, see also Section 2.3.1. Especially, the antennas operating in the lower UHF band have inherently low electromagnetic isolation (concept introduced in [79]) due to the strong coupling through the half-wave mode of the chassis [**II**]. In the above-presented design, the total isolation between the DTV and E-GSM antennas is anyway at least 22 dB but it is mainly maintained by the matching circuits which operate also as filters since the systems have certain frequency separation – i.e., the electromagnetic isolation between the antennas is only a couple of decibels in magnitude. However, this 22 dB is not enough according to the DVB-H specification (61 dB is required) [42], [43]. Thus, one of the future's important research topics is to study methods how to provide a large enough isolation between the antennas. This requires the optimisation of the antenna elements (better electromagnetic isolation) and the circuit technology (better filtering with small enough insertion loss). Possible means are the relocating/reshaping of the CCEs, neutralisation lines and filters (e.g., SAW technology). The issue is further elaborated in [**II**].

CCE-based DTV antennas have also aroused interest among industrial antenna manufacturers, such as Pulse Engineering, who have implemented their own internal DTV antenna based on the CCE antenna concept [80].

3.3.4 Tuneable antennas based on capacitive coupling elements

The motivation for tuneable antennas is that it is very challenging to implement resonant-type antenna elements (such as PIFAs or IFAs) for each of the frequency bands required in the multi-system handheld devices of the future. In addition, the upper limit of the available impedance bandwidth is approached with the studied passive CCE antenna structures in the lower UHF band. Thus, the possibility to cover separate frequency bands and/or large virtual impedance bandwidths based on a single frequency-tuneable antenna element is a very tempting option. The capacitive coupling element concept with tuneable matching circuitry suits especially well for the implementation of frequency-tuneable antennas [26].

Since the CCE is non-resonant (see Fig. 4) and the resonant frequency of the antenna is chosen with a matching circuit, a tuneable antenna based on one single CCE can be implemented, in principle, rather easily by using an adaptive matching circuitry. As is presented in Section 2.2.2, the typical ways to implement an adaptive matching circuitry are to use either a) electrically adjustable tuning component(s), such as a varactor, in a part of the matching circuit, or b) switching between separate parallel matching circuits, see the general tuning-circuit topologies in Fig. 12.

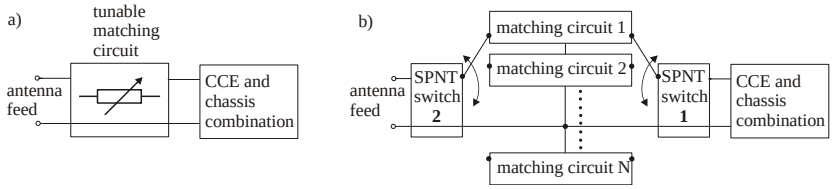

Fig. 12. General tuning-circuit topologies for frequency-tuneable CCE antennas based on a) electrically adjustable tuning component(s) in a part of the matching circuit, and b) switching between parallel matching circuits.

To the author's knowledge, the first tuneable CCE-based antenna structure was introduced in [28], where a broadband lower UHF-band digital television antenna was implemented. The prototype consists of two parallel matching circuits (each for adjacent lower and upper sub-bands) and two SPDT PHEMT GaAs semiconductor RF switches, see the general topology in Fig. 12b. Even though the DVB-H realised gain specification was just fulfilled, the matching and realised gain measurements revealed several practical problems, such as poor isolation of the OFF-branch and relatively high losses of the RF switches, and unexpected impedance behaviour of the antenna. A presumable reason for these problems was that the RF switches were placed in a non-50-Ω impedance environment, which is typical for CCE antennas (see Fig. 4), but far from optimal for RF switches that are typically intended to operate in a 50-Ω impedance environment. Thus, it is very important to pay attention to the load impedance where the switch is attached to. A similar two-stage tuning concept was designed with simulations in the 0.9-GHz band in [27].

The first systematic study on the implementation of tuneable CCE-based antennas was presented in [29], [30]. A dual-band operation at 0.9 and 1.8 GHz frequency bands was demonstrated based on one CCE, two parallel matching circuits and two SPDT PHEMT semiconductor RF switches – see the general tuning-circuit topology in Fig. 12b. Methods to optimise the losses in the tuning circuit were studied. However, the switches caused relative large losses (about 2 dB), especially in the switch next to the CCE (switch 1 in Fig. 12b). In addition, the tuning circuit was not at all optimised

from the distortion point of view, and thus the measured IMD_3 (intermodulation distortion of the third harmonic) was as high as -13 dBc at 0.9 GHz (two-tone test, 30 dBm/tone).

The systematic loss and distortion studies of the semiconductor switch-based tuneable CCE antennas were continued in [**III**]. The reason for relatively large losses in the switch directly next to the CCE (see Fig. 12b) is that the effective radiation resistance R_{rad} of the unmatched CCE is typically relatively small, see Fig. 7a, and since the semiconductor switch introduces a loss resistor R_{loss}, typically a few ohms of magnitude, the radiation efficiency decreases significantly (2.7). Thus, the low-resistance environment is not optimal from the losses point of view. The improvement in the radiation efficiency requires either better switches (lower ohmic losses) or placing the switch in a high-resistance location. The latter can be implemented by manipulating the impedance of the CCE antenna. For example, the effective resistance of the CCE was manipulated (or rather optimised) with a parallel inductor in [29], [30]. However, the optimal impedance environment is rather challenging to implement at several frequency bands at the same time.

The tuning circuit cannot be optimised from the losses point of view only. When the distortion of a semiconductor switch is taken into account, it shows that the high-resistance (or generally high-impedance) location is not optimal either. It has been suggested already in [18] and systematically studied in [**III**] that there is a strong correlation between the load impedance of a semiconductor RF switch and the distortion: the higher the on-port impedance (i.e., voltage) of the switch is, the higher is the distortion. Concluding the discussion above, there is obviously a trade-off between the losses and distortion caused by the semiconductor RF switch. In [**III**] the above-discussed problem was avoided by totally omitting the switch next to the CCE. It was demonstrated that the lossy, non-linear semiconductor RF switch (switch 1 in Fig. 12b) is possible to replace with passive reactive components, which comprise a filter between the parallel matching circuits, without loss of performance. Actually, the efficiencies were improved up to 20%-units and the IMD_3 up to 36 dB at 0.9 GHz compared to the two-switch prototype in [30]. Generally, a similar topology could be applied to any pair of frequency bands, which have just sufficient relative frequency separation.

Later in [81], a two-switch tuning circuit (see Fig. 12b) was implemented based on micro-electro-mechanical-system (MEMS) technology. The ohmic losses were demonstrated to be on the same level as in the antenna in [**III**], where only one semiconductor RF switch was used, but the linearity

properties of the MEMS switches were superior compared to the semiconductor-switch implementations. However, it is a well-known fact that the RF MEMS switches need still to be improved in terms of the costs and reliability before they can be used in commercial mobile terminals [82], [83]. In addition, a MEMS-switched tuneable mobile terminal antenna is introduced in [84].

The general design aspects of "continuously" frequency-tuneable CCE antennas based on an electrically adjustable tuning components as a part of the matching circuit (see Fig. 12a) were presented in [46]. However, practical implementation of the tuneable matching circuit was not proposed. In [25], [85] and [86], wideband frequency tuning of CCE antennas in the UHF band was implemented based on a variable capacitance, but the practical implementation with a varactor was still omitted. In [24], a continuously tuneable lower UHF-band receiving antenna, for instance, for digital television reception, was implemented based on varactors in a part of the matching circuit. The practical implementation with proper distortion analysis was also presented.

In [87], an antenna consisting of a CCE and several parallel matching circuits was implemented on a low-temperature co-fired ceramic (LTCC) component. Unfortunately, the switching between the matching circuits was not yet implemented.

Concluding all the discussions above, it is obvious that the tuneable CCE-based antennas can provide a wide tuning range in the UHF band. The challenges with losses and distortion of the semiconductor components set practical limitations to the implementation of frequency-tuneable antennas. In future, the expected development of the tuning components, such as MEMS switches, semiconductor switches and varactors, enables improved feasibility of the frequency-tuneable antennas. This would make possible that instead of several separate antenna elements, the handheld multisystem radios of the future might include only a couple of frequency-tuneable antenna elements (possible CCEs) for several required frequency bands [1].

3.4 Antennas with direct feed

3.4.1 Basic concept and review on existing solutions

The basic idea behind the direct feed antennas is to galvanically excite the radiative common mode currents of the chassis wavemode(s). This way the coupling to the chassis wavemode(s) becomes relatively strong as well as the volume occupied by the "antenna" might decrease fairly much. Very strong coupling could be achieved by splitting the chassis in the middle into

two parts and then feed the antenna between the parts, such as studied in [88]. However, the chassis cannot be easily separated into two parts. Hence, the feed is implemented over an impedance discontinuity, such as a slot (with a strip connecting two parts), see the example in Fig. 13a.

The IE3D-simulated fundamental impedance of the direct feed antenna of Fig. 13a is shown in Fig. 13b. Such as in the case of CCE antennas, the matching at the selected frequency band can be done with an external matching circuit attached to the feed. The coupling to the chassis wavemodes is created through the transmission-line-type (or differential mode) wavemode of the slot. The effect of the half- and full-wave chassis major axis modes can be seen in the input impedance at 1.2 and 2.6 GHz (compare with the impedance of the CCE-based antenna in Fig. 4b). The strong resonance at 3.1-3.2 GHz is the major axis one-and-a-half wavemode of the chassis. The principal current distributions at the chassis resonant frequencies are shown in Fig. 14. The minor axis wavemodes are not excited since the orientation of the slot and the feed cannot effectively excite the common mode current distributions of the minor axis of the chassis. The slot itself does not remarkably contribute to the radiation since the transmission-line-type currents, which are very close to each other in wavelengths, flow to opposite directions and their effect is thus cancelled in the far field. On the other hand, the slot resonates when its electrical length is a quarter-wavelength (at about 1.8 GHz) but at that frequency its impedance is very high [89]. The chassis has also the anti-resonance around 1.8 GHz and thus the whole direct feed antenna structure has the anti-resonance at about 1.8 GHz, see Fig. 13b.

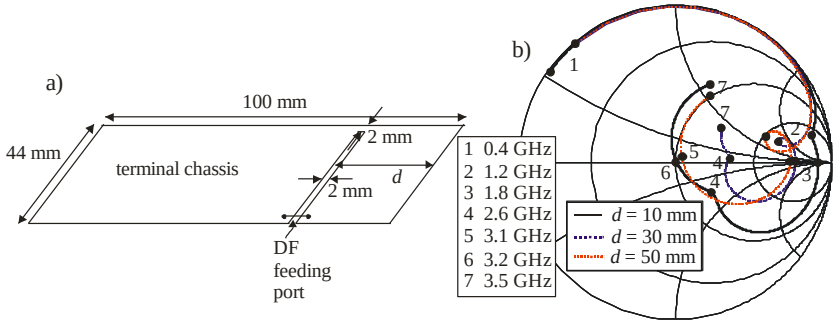

Fig. 13. a) Basic direct feed (DF) structure and b) its IE3D-simulated impedance on the Smith chart with different *d*.

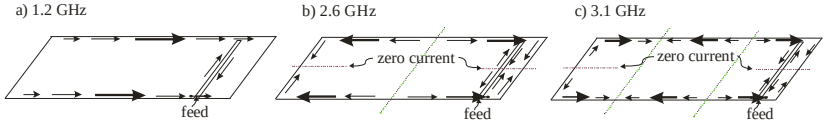

Fig. 14. Principal current distributions of the basic direct feed structure at the resonant frequencies a) 1.2, b) 2.6 and c) 3.1 GHz of the chassis.

As in the case of CCE antennas, the location of the feed significantly affects the excitation of the chassis wavemodes of the direct feed antennas, and thus it affects also the available impedance bandwidth of the antenna. The strongest coupling to the half-wave mode at 1.2 GHz (and consequently the smallest radiation quality factor) takes place when the feed is placed in the mid-point of the major axis (d = 50 mm). In Fig. 13b that can be seen from the size of the "loop" at 1.2 GHz, indicating that the strongest coupling (largest loop) to the half-wave mode is achieved when d = 50 mm. Instead, in the case of d = 10 mm, only a small "dip" indicating lower coupling can be noticed. The reason for this is the electric current distribution of the chassis: the current maximum of the half-wave mode is located in the mid-point of the major axis, see Fig. 14. The coupling is low to the full-wave mode at 2.6 GHz when d = 50 mm (no loop/dip at 2.6 GHz) and to the one-and-a-half wave mode when d = 30 mm. The explanation is the minimum/zero of the current distribution, see also Fig. 14.

Since the height of the direct feed structure is extremely low, the antenna suits, in principle, especially well for low-profile platforms. The direct feed would also suit particularly well for mobile terminals which "naturally" contain a slot. For example, in clamshell/folder terminals there is a slot between the lower and upper parts and thus, the direct feed antenna might be implemented across the slot. The feed and strip can be implemented within the hinges.

One challenge in the direct feed antennas is that a floating metallic patch, such as the display or battery, above the feeding slot introduces a large capacitance across the slot, and thus the unloaded quality factor increases and consequently the impedance bandwidth decreases. The effect of the metallic patch placed above the feeding slot of a direct feed antenna is studied in [90]. A short circuiting of the patch further decreases the bandwidth. However, when the short circuits at selected locations were replaced with inductors, which still provide DC grounding of the patch, the loss of the bandwidth due to the metallic patch is possible to partly recover. Concluding the discussions above, a metallic patch covering the slot can be made possible by partly sacrificing the impedance bandwidth of the antenna.

Another challenge is increased specific absorption rate values compared to antennas based on an actual antenna element, such as PIFA or CCE. It is well-known that the SAR values of mobile terminal antennas are strongly affected by the chassis wavemodes in the UHF band [64], [68], [69]. Since the direct feed antennas have relatively strong coupling to the chassis wavemodes and especially strong electric fields across the slot, the local SAR values can be expected to increase compared to CCE antennas. That might be one reason why the direct feed antennas have not yet been widely introduced in commercial mobile terminals. However, the high local SAR might not impede receiving antennas.

Several research teams around the world have studied direct feed concept independently at the same time. The direct-feed principle was introduced by a Spanish research team in [91]. A very wideband operation in the UHF band was possible by strong excitation of the chassis wavemodes. A research team in Taiwan introduced their direct feed antenna for clamshell-type terminals in [53]. The application example is lower UHF-band digital television receiver. A sort of direct feed antenna is introduced by a German research team in [92]. Even though they call the concept "inductive coupling", the operational principle is greatly the same as in the direct feed antennas introduced above. The application examples are for 1- and 2-GHz cellular systems and a lower UHF-band digital television receiver. The direct feed-based antenna structures introduced by the research team of the author of this thesis are presented in articles [**IV**], [**V**] and shortly introduced in this chapter. A very wideband direct feed antenna for mobile terminals is introduced by a Chinese researcher as well [93], [94].

A similar antenna to the one shown in Fig. 13a (with d = 50 mm and lumped-element L-section matching circuit to match the antenna around 0.9 GHz), designed and built by the author of this thesis, won the "*Small Antenna Contest*" (organised by the European antenna research community "Antenna Center of Excellence" ACE) in the single-band antenna category in 2007 [95]. The antennas were ranked by the total efficiency across 0.88-0.96 GHz. The total efficiency of the winning antenna prototype is better than 74%.

3.4.2 Implementation of broadband lower UHF-band receiving antenna – application example digital television receiver system

The implementation of a broadband lower UHF-band receiving antenna based on the direct feed for a tablet-size terminal is studied and demonstrated in [**IV**]. As was presented in the previous section, the most optimal place of the feeding slot from the impedance bandwidth point of

view would be in the mid-point of the major axis of the chassis. In this case, we prefer to allocate the middle of the terminal for the display, not the feeding slot, see Fig. 15. Another slot on the chassis is introduced to lengthen the current path and thus decrease the resonant frequency of the half-wave mode of the chassis. This is useful from the impedance bandwidth point of view, as it was told in Section 3.2. In a case where the distance between the slots is 70 mm, the half-wave mode resonance is at 0.675 GHz. The display and battery can be placed between the slots and thus they do not significantly affect the operation of the antenna. A method how to avoid the use of another slot (and consequently enable the use of a larger-size display) will be presented in the next section.

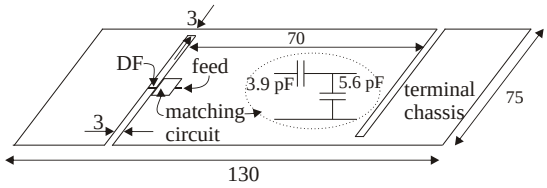

Fig. 15. Direct feed-based broadband lower UHF-band receiver antenna.

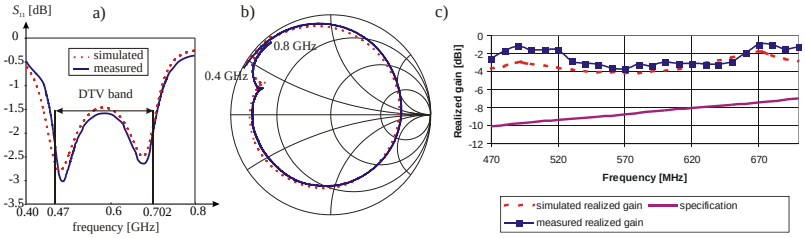

Fig. 16. Simulated and measured reflection coefficient a) in the Cartesian coordinate system and b) on the Smith chart, and c) simulated and measured realised gain.

The reflection coefficient of the antenna structure is shown in Fig. 16ab. As can be seen, at least about 1.5-dB return loss is achieved across the DTV band 0.47 - 0.702 GHz (when this prototype was designed, the DTV band was limited up to 0.702 GHz if E-GSM was used in the same terminal). The justifications for the moderate matching level are given in Section 3.3.3 and **[II].** Although the matching circuit becomes single-resonant, the frequency response of the reflection coefficient is dual-resonant due to the chassis wavemode at 0.675 GHz. However, one can see from the Smith chart presentation in Fig. 16b that the dual-resonant operation is far from optimal [96]. The main problem is that instead of having the optimal double loop around the Smith chart centre, there is only a small dip at 0.675 GHz indicating clearly too weak coupling to the chassis wavemode (compare with Fig. 11b). The reason for that is the location of the feed slot far away from the optimum location, the middle of the chassis. The second

problem is that the resonant frequency of the chassis wavemode (at 0.675 GHz) is not equal to the centre frequency of the DTV band (0.586 GHz). Nevertheless, the performance of the antenna is very good, 4 dB above the realised-gain specification, see Fig. 16c. When comparing to the corresponding CCE antenna in Section 3.3.3 (Fig. 10 and Fig. 11), both the antennas can provide roughly the same realised-gain performance. The directional pattern is a dipole-type doughnut since the half-wave mode of the chassis is the main radiator. The advantage of the direct feed solution over the CCE is the zero-height structure but the challenge is the need for the slot(s). Further studies, for example, on the user hand effect of this direct feed antenna are performed in [97], [98].

A lower UHF-band direct feed antenna (with only one slot) for an open clamshell/folder terminal is simulated in [97]. With the lossless antenna structure, whose overall size in the open position is 165 mm × 40 mm [length × width], the performance margin to the realised-gain specification is at least 6 dB. The reason for the improved performance compared to the antenna in Fig. 15 is a clearly longer chassis (165 mm versus 130 mm) which is especially useful below 1 GHz, see Section 3.2.

3.4.3 Optimised direct feed

The motivation for the "optimised direct feed" is to try to maximise the impedance bandwidth of a mobile terminal antenna whilst the size of the "antenna" is minimised. As it was described in the previous section, the operation of the antenna of Fig. 15 was not optimal from the bandwidth point of view. Thus, the resonant frequency of the chassis could be decreased by introducing more slots in the chassis. However, the use of additional slots may not always be feasible since the printed circuit area is needed for the electronics. Secondly, conductive elements (such as display and/or battery) above the slots complicate the operation of the antenna, as explained in Section 3.4.1. Instead of using additional slots, it is proposed in [99], [**V**] to replace the strip of the feeding slot with an inductor in order to tune the resonant frequency of the chassis to the operating frequency band, see Fig. 17a. The inductor still provides the DC grounding between the segments of the chassis. In the optimal case the inductor value L is chosen so that the resonant frequency of the combination of the feed structure and chassis equals the centre frequency of the operating band. The coupling between the feed structure and the chassis dominant wavemode can be optimised by modifying the length l of the feed structure [99], [**V**], see Fig. 17a. The studied antenna concept enables very broad impedance bandwidths, especially in the lower UHF band, see Fig. 18. The antenna

presented in the previous section (Fig. 13) could also be further optimised based on the principle introduced in this section.

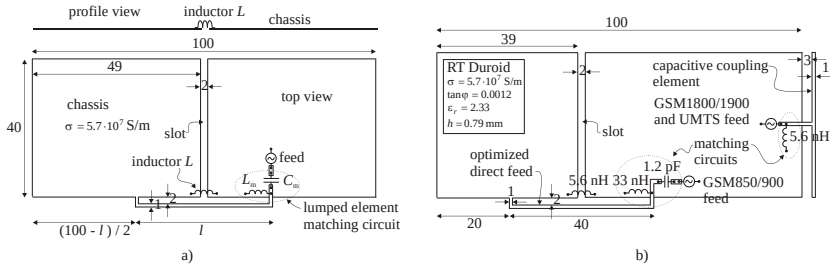

Fig. 17 a) Principle of the optimised direct feed, and b) a sketch of the dual-band prototype antenna.

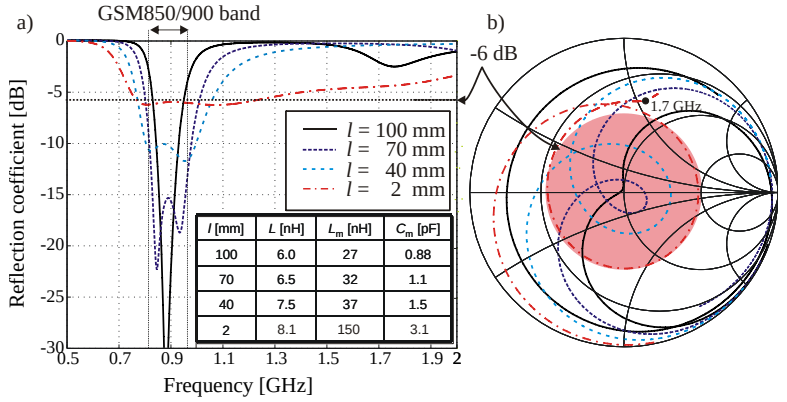

Fig. 18. Effect of the length *l* of the feed structure of the antenna in Fig. 17a on the matching a) in the Cartesian coordinate system and b) on the Smith chart.

A dual-band (lower band at 0.8-1 GHz and upper band at 1.7-2.1 GHz) antenna prototype for mobile terminals was designed, built, and measured in [**V**]. The antenna functionality for the lower band was implemented using the optimised direct feed structure and for the upper band using capacitive coupling element, see Fig. 17b. The prototype has excellent matching and radiation efficiency at all bands. In addition, the bandwidth of the upper band could easily be broadened with a multi-resonant matching circuit. However, the drawback of the optimised direct feed antenna is clearly increased (27%) specific absorption rate and lower radiation efficiency in the talk position compared to the CCE-based antenna (similar to shown in Fig. 4a). Especially, the high SAR is concentrated in the vicinity of the 5.6-nH inductor. However, one should note that the prototype was optimised from the bandwidth point of view only, and thus the optimisation of the SAR is an interesting research topic in the future. The directional pattern of the antenna at 0.9 GHz is a dipole-type doughnut since the half-wave mode of the chassis is the main radiator.

4 User interaction of compact coupling-based antennas

4.1 General

It is a well-known fact that lossy dielectric material (such as a user) within the reactive near fields, which typically extends to a distance of $\lambda_0/2\pi$ from the surface of a small antenna, affects the matching, efficiency and directional pattern of a mobile terminal antenna [100]-[107]. This is a very important research topic because the phenomenon is not yet comprehensively understood. In addition, mobile terminals are almost always used in the close vicinity of the user and thus the effect of the user needs to be taken into account in the design of the antennas as well as in the design of the respective radio system. However, the complete ”removal” of the user effect phenomenon is challenging because it takes place within the inherent reactive near fields, and on the other hand it is impossible to totally eliminate the near fields since otherwise the antenna would not radiate.

Fig. 19 shows a measured example which relates to the effect of a lossy dielectric cube on the input impedance of a matched capacitive coupling element (CCE) antenna of Fig. 4a. The cube is placed in three different positions with respect to the antenna at a 3-mm distance from the structure, see Fig. 19a. At 0.95 GHz the outer boundary of the reactive near fields extends to about 50 mm ($\lambda_0/2\pi$) from the surface of the antenna and thus the cube is clearly within the near fields of the antenna. It can be seen that the resonant frequency of the antenna can either increase, decrease or stay roughly the same depending on the location of the dielectric cube, see Fig. 19b. This phenomenon will be further studied in Section 4.2. The user hand effect on the CCE-based broadband lower UHF-band receiving antenna (see Fig. 10) will be studied in Section 4.3. The methods for compensating the effect of the user will be discussed as well.

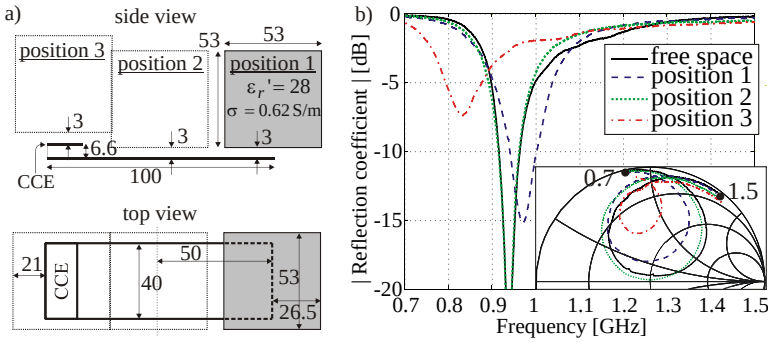

Fig. 19. a) Dielectric cube placed in three different locations around the prototype antenna of Fig. 4a, and b) the measured reflection coefficient of the antenna matched in free space at 0.95 GHz when loaded by the dielectric cube. Dimensions are in mm.

On the other hand, it is not only the user who affects the antenna, but also vice versa: the reactive near fields can affect the user. The specific absorption rate (SAR) is used to measure the power absorption by the human tissue, see Sections 2.1.4 and 2.3.1. The strong reactive near fields of the antennas can also cause electromagnetic compatibility problems, for example, by disturbing the operation of the hearing aid of the user [16]. Thus it would be very important to be able to control the reactive near fields of the antennas without worsening the far-field radiation properties. The methods how to modify the near fields of mobile terminal antennas will be discussed in Section 4.4.

4.2 Wavemode modelling-based analysis

There are several papers studying the impedance and efficiency variations of mobile terminal antennas in the presence of the user. For example, in [103] it has been shown that lossy dielectric material close to the antenna element (PIFA) is a much greater problem than the same material close to the chassis. The same conclusion can be drawn also from Fig. 19. In addition, it has been shown that the fundamental impedance of the antenna becomes more resistive and inductive due to the presence of lossy dielectric material [103], [105], [**VII**]. The impedance variations of the antennas have been well-described but the detailed explanations of the behaviour of the antenna impedance have not been given before. That will be done in this section and [**VI**].

It has been presented in [**VI**] that a better qualitative understanding of the behaviour of the antenna impedance and efficiency due to the dielectric material placed into the reactive near fields of the antenna can be obtained by applying a coupled resonator-based equivalent circuit model of a CCE-

based mobile terminal antenna (see Section 3.3.2), with modelling the user body effect separately for each wavemode of the circuit model. Even though measurements and EM simulations have a great importance in the user body effect studies, the proposed circuit-theoretical study separates the analysis into smaller parts enabling profound understanding of the impedance and efficiency variations caused by the presence the dielectric material in the reactive near fields of the antenna.

The effect of the dielectric material placed into the reactive near field of the CCE-based mobile terminal antenna is modelled by introducing additional parasitic components to each RLC resonator of the circuit model shown in Fig. 6 in such a way that certain realistic changes of the resonant frequency and quality factor are implemented. The decrease of the resonant frequency of each wavemode can be implemented with a parasitic capacitor C_u placed parallel to the free space capacitor of the RLC resonator circuits, see Fig. 20. The Q value of each resonator at the resonant frequency can be controlled by introducing a parasitic resistor R_u. The detailed explanations of the modifications of the resonator circuits are given in **[VI]**. The component values of the additional components can be determined based electromagnetic simulations or in some cases with the help of the perturbation theory [106].

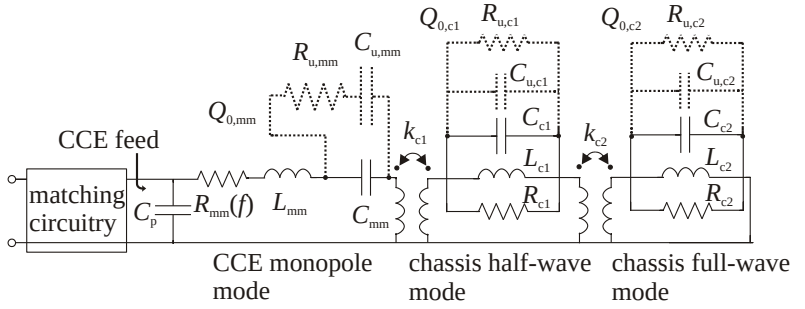

Fig. 20. Modification of the RLC resonator circuits of CCE monopole mode and chassis wavemodes due to lossy dielectric material placed into the near fields of the respective wavemode. Q_o is the new unloaded quality factor of the respective wavemode.

The effect of lossless dielectric material close to the chassis on the fundamental impedance variations of the unmatched CCE antenna is studied. For example, this condition corresponds to the case when the user's palm is located in the (open) end of the chassis. The total resistance and reactance (without the matching circuit) derived from the equivalent circuit model by applying $C_{u,c1}$ and $C_{u,c2}$ (thus $f_{r,c1}$ and $f_{r,c2}$ decrease) are shown in Fig. 21. The "perturbed" resistance and reactance are compared with those in the free space. Since the resistive losses are not included, the

total resistance can be considered to represent only the "losses" due to the radiation.

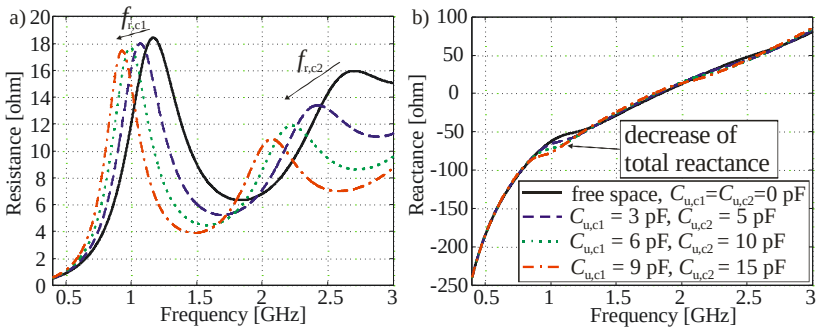

Fig. 21. Effect of the shift of the resonant frequencies of the chassis wavemodes on the total a) resistance and b) reactance of the circuit model.

Firstly, it can be seen in Fig. 21a that the decrease of each resonant frequency of the chassis wavemodes has a significant influence on the total resistance behaviour. This happens because the total resistance of the CCE antenna is mainly dictated by the chassis wavemodes in the UHF band, see Fig. 7b. Especially, the total radiation resistance significantly increases below 1 GHz, i.e., at the frequencies below the half-wave mode of the chassis. Possible benefits of this phenomenon on the matching and efficiency will be handled in the next section. Secondly, the total reactance in Fig. 21b is significantly affected only around the resonant frequency of the first order chassis wavemode (at the 1-GHz range). This happens because the reactance of the CCE mainly determines the total reactance behaviour of the antenna, and the chassis wavemodes can thus affect the reactance only around the chassis resonances, see Fig. 7b again.

Next, the effect of the lossless dielectric material loading the CCE monopole mode is investigated. That condition can take place when the user's finger or hand is close to the CCE. The total resistance and reactance of the circuit model of Fig. 20 after applying $C_{u,mm}$ are shown in Fig. 22. Contrary to the results of the previous paragraph, the decrease of the fundamental frequency $f_{r,mm}$ of the CCE monopole mode has a relatively large influence on the total reactance behaviour in the whole UHF band. The explanation is the same as in the previous section: the CCE reactance dictates the total reactance of the whole antenna. It can also be noticed that the impedance always changes to the inductive direction when the CCE monopole mode is loaded, as described also in [103]. Since the reactance increases significantly, it can be expected that the resonant frequency of a matched antenna would decrease correspondingly.

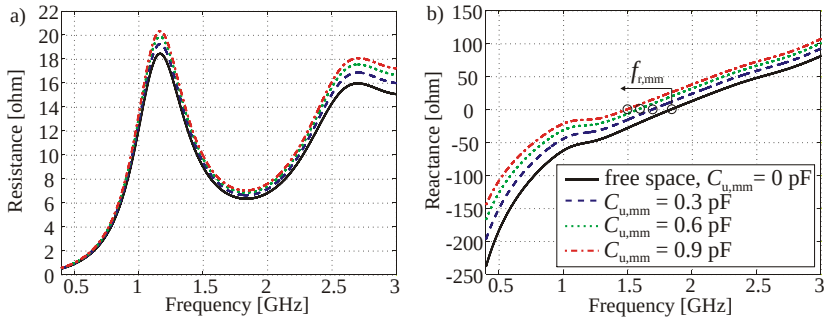

Fig. 22. Effect of the shift of the fundamental frequency of the CCE monopole mode on the total a) resistance and b) reactance of the circuit model.

Finally, the effect of simultaneous loading of the first chassis wavemode and the CCE monopole mode on a matched CCE antenna of Fig. 4a is studied with an example shown in Fig. 23. If only the chassis wavemode is loaded with $C_{u,c1}$, the resonant frequency of the matched antenna is tuned upwards. This happens because the change of the chassis resonant frequency decreases the antenna reactance around 1 GHz; see Fig. 21b, and thus the resonance is shifted upwards in frequency. Increasing the resistive losses $R_{u,c1}$ on the chassis wavemode partly compensates the frequency shift caused by the effect of the capacitance $C_{u,c1}$. The case of only loading the chassis wavemode can be associated with the "position 1" of the measured example in Fig. 19. Then, if dielectric loading on the monopole mode is added ($C_{u,mm}$), the resonant frequency of the CCE antenna quickly decreases. The reason is the significant increase of the total reactance, see Fig. 22b. Adding resistive losses on the monopole mode ($R_{u,mm}$) does not change the frequency anymore, but it makes the matching level worse by shrinking the matching loop on the Smith chart. A similar effect can also be seen in the measured example, see "position 3" in Fig. 19. This impedance behaviour can be understood with basic resonator theory: a critically-coupled resonator becomes undercoupled when the internal losses (here resistive losses) are increased.

Rough qualitative radiation efficiency estimations can also be performed based on the circuit model. After applying R_u it can easily be calculated how much resistive losses are generated in each wavemode compared to the radiation "losses". The results, which are not shown here in detail, indicate that the resistive losses in the CCE monopole mode caused by $R_{u,mm}$ have a much larger effect on the overall radiation efficiency than the losses in the chassis wavemodes caused by $R_{u,c1}$ and $R_{u,c2}$, especially at the frequencies lower than the half-wave mode of the chassis. The result is also supported by the impedance behaviour on the Smith chart in Fig. 19 and Fig. 23,

where the fairly small impedance loop indicates remarkably increased resistive losses and, consequently, the clearly reduced radiation efficiency of the antenna. The reason for this is that the resistive losses in the CCE monopole mode affect relatively much the total resistance since it is very small at the frequencies below the half-wave mode of the chassis (see Fig. 7b) and thus the radiation efficiency decreases fairly much according to (2.7). This is also typical for resonators having a relatively high radiation Q value, such as the CCE monopole mode [**I**] (2.3)**.** On the other hand, the resistive losses in the chassis wavemodes do not affect the total resistance (and consequently the radiation efficiency) as much as those in the CCE monopole mode since the radiation Q values of the chassis wavemodes are rather low. At the frequencies above the half-wave mode of the chassis the effect of the resistive losses in the CCE monopole mode on the overall radiation efficiency becomes clearly smaller. These results have been confirmed with EM simulations.

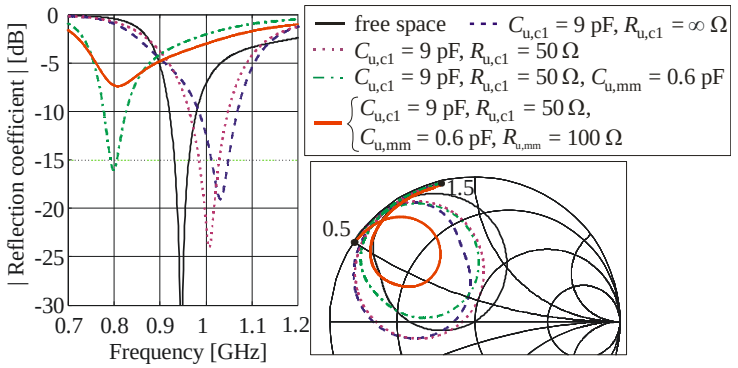

Fig. 23. Effect of the simultaneous loading of the wavemodes on the matching at 0.95 GHz.

4.3 User effect of lower UHF-band CCE-based antennas

In this section and in paper [**VII**], the operation of the earlier presented CCE-based lower UHF-band receiving antenna (see Fig. 10a) in typical use positions is investigated. Since users are increasingly using mobile terminals for data services, the focus is shifting from the talk mode to the data mode and thus the effect of the user's hands on the antenna operation has much greater importance than earlier. Therefore, the main objective of [**VII**] is to study the antenna performance in the presence of the user's hands. The results are not restricted only to the examined antenna, but they aim to gain a general understanding on the user's hand effect within the lower UHF band.

Fig. 24 shows the studied CCE antenna structure in the landscape browsing grip, but other use positions (portrait palm and end grips) are also covered

in [**VII**]. The studied parameters are matching (Fig. 25 and Fig. 26a), radiation efficiency (Fig. 27a), total efficiency (Fig. 26b and Fig. 27b), and far field directional pattern. They are studied with electromagnetic simulations and verified with measurements. In order to make the interpretation of the SEMCAD simulation results more straightforward, the simulations are performed with a lossless antenna model. The user's hands are modelled with the lossy, homogenous, fully-posable human hand phantoms available in SEMCAD, see Fig. 24a. The measurements are performed with the real hands of a test person, see Fig. 24b. One should note that not exactly the same things are simulated and measured, and thus direct and precise comparison of the numeric values of the results is not possible to perform. Instead, one should observe the trends between the simulated and measured results. See further details of the research methods in [**VII**].

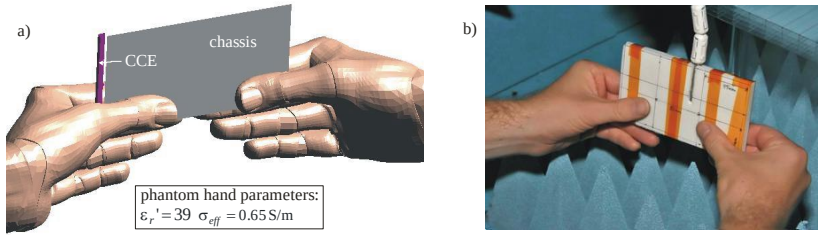

Fig. 24. Studied antenna in the landscape browsing grip, a) in the SEMCAD simulator and b) in the impedance measurements.

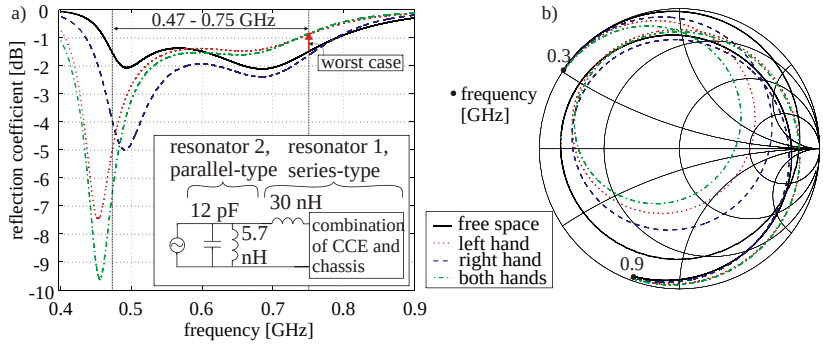

Fig. 25. Effect of the user's hands on the a) matching and b) input impedance of the antenna with the matching circuit (simulated).

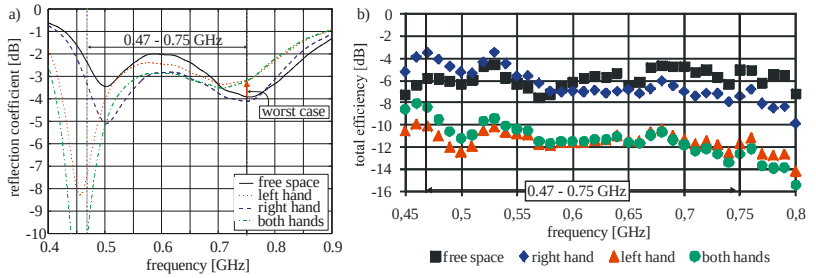

Fig. 26. Effect of the user's hands on the a) matching and b) total efficiency of the prototype antenna (measured).

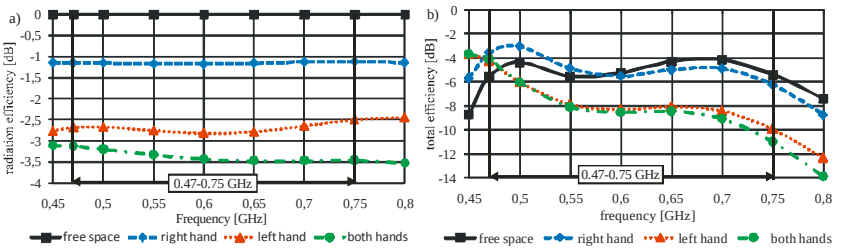

Fig. 27. Simulated a) radiation and b) total efficiency of the antenna. The dots show the simulated frequencies.

Firstly, the fundamental (unmatched) impedance behaviour of the antenna in the user's hand grip presented in [**VII**] is fully supported by the circuit-model approach presented in the previous section. Secondly, in the matched case (Fig. 25 and Fig. 26a) the impedance band is tuned downwards in frequency when the hand is close to the CCE (left hand case), compare also with Fig. 19 and Fig. 23. That happens since the total reactance increases due to the fact that the resonant frequency of the CCE monopole mode decreases, as explained in the previous section in Fig. 22b. On the Smith chart in Fig. 25b the impedance operation becomes also non-optimal (asymmetrical inner loop with respect to the centre of the Smith chart according to [96]) since the resonant frequency of resonator 1 (see Fig. 25a) changes significantly due to the hand. The matching efficiency (2.8) in the simulated case in Fig. 25 decreases 1.9 dB in the worst case at 0.75 GHz. In the corresponding measured case, the degradation of the matching efficiency is smaller since the impedance band is somewhat larger on the upper edge of the band. When the hand is at the opposite end to the element (right hand case) and loads only the chassis wavemodes, the impedance band stays essentially unchanged. This can be explained according to Fig. 21b since the reactance is also unchanged at the frequencies lower than the resonant frequency of the half-wave mode (in this antenna $f_{r,c1}$ = 0.9 GHz). Actually, the matching level is even improved at the whole band since the total resistance of the antenna increases; see the

reason in Fig. 21a. The same effect is reported also in [108]. The same trends of the matching behaviour can be noticed with portrait palm and end grips in [**VII**].

The radiation efficiency (2.7) behaviour (in Fig. 27a) follows the trend explained in the end of the previous section: when the hand loads only the chassis half-wave wavemode (right hand case), the resistive losses are clearly lower than the losses caused by the loading of the CCE monopole mode (left hand and both hands case). The total efficiency (2.11) behaviour (in Fig. 26b and Fig. 27b) is interesting: it can even increase in some cases (right hand). This happens since the matching efficiency improvement more than compensates the radiation efficiency degradation. This "positive hand effect" is reported at the 0.9-GHz band also in [108]. The hand close to the CCE has the most effect on the antenna operation at 0.47-0.75 GHz; several of dBs losses compared to the free space case can be expected. The simulated realised-gain directional patterns are shown in [**VII**]. Generally it can be concluded that the distortion of the directional patterns due to the user's hands seems not very problematic since the pattern remains rather omnidirectional.

The performed studies give also insight how to compensate the effect of the user. Possible ways would be to:

1) try to place the antenna element in such a location that the user's hand does not cause too heavy loading,
2) match the antenna over a wide enough impedance bandwidth so that the detuning does not result in significant degradation of matching efficiency (see Fig. 26a), or
3) use an adaptive matching circuitry with a matching detector [109], [110] (adaptive matching is related to frequency-tuneable antennas, see Section 3.3.4), or
4) use multiple antenna elements, such as in [111], and select the element in use based on the location of the hand(s) [112].

4.4 Near-field control – focus on hearing-aid compatibility

Since an electrically small antenna stores inherently much energy in the reactive near fields, the strengths of the electric and magnetic fields become rather strong around the antenna structure. Fig. 28 shows the SEMCAD-simulated electric and magnetic field peak strengths (1-W transmit power) of the CCE antenna of Fig. 4a at 15-mm distance from the surface of the antenna structure, see also Fig. 3a. It can be seen that the strong electric fields exist not only around the CCE but also around the open end of the

chassis (opposite to the antenna element). It has been explained in [**VII**] that the strong electric fields in the open end are caused by the minimum/zero of the common mode current distributions of the chassis wavemodes, see also Section 3.3.1. The same phenomenon has later been studied in [113], [114].

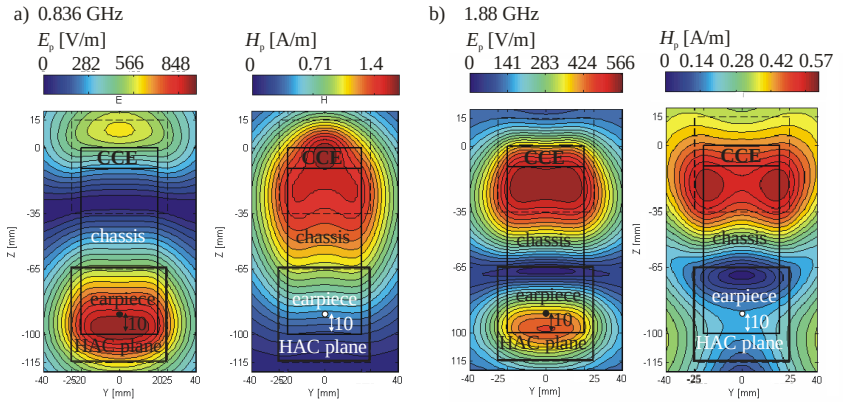

Fig. 28. Electric and magnetic near fields of the CCE antenna of Fig. 4a at a 15-mm distance from the surface of the antenna structure at a) 0.836 GHz and b) 1.88 GHz.

One challenge of the strong reactive near fields is related to the hearing-aid compatibility (HAC); the problem is well-explained in [115], see also Section 2.1.4. The simulated field strength values for this fairly ideal full-metal design in Fig. 28 are very high and actually not even close to the limits of the specifications given in the HAC standard M3 (articulation weighting factor -5 dB) [**VIII**], [16]. Thus, it would be very important to be able to somehow reduce the field strengths on the HAC plane which is a 50-mm square around the earpiece of a mobile terminal at a 15-mm distance from the surface of the phone. In Fig. 28 the CCE is defined to be bottom-located and the HAC plane is shown in the open end of the chassis.

In order to reduce the field strengths on the HAC plane, the typical common mode current distribution of the chassis needs to be somehow manipulated, especially in the chassis parts above the HAC plane. One should however note that the manipulation of the common mode currents, which significantly contribute to the radiation in the UHF band, affects the resonant frequency and radiation Q value of the chassis wavemode(s) and thus also the total radiation resistance, available impedance bandwidth and specific absorption rate values of the antenna. The effect can however be favourable if the chassis wavemodes are manipulated suitably relative to the used frequency band.

In the open literature, there exist some solutions which can be used to reduce the near fields of mobile terminal antennas to fulfill the HAC standard. In [116], a dual-element phased antenna system is used to create differential mode current distributions on the edges of the chassis. This antenna system enables clearly reduced near fields in the open end (opposite to the antenna elements) of the chassis compared to the antenna element(s) which excite the common mode current distributions, such as in Fig. 28. Similar operation can also be implemented with a loop antenna [116].

Another option to reduce the near fields on the HAC plane is to electromagnetically isolate the segmented part of the chassis above the HAC plane from the radiating part of the chassis or the antenna. In [117], the upper part of the chassis of a clamshell/folder-type terminal is isolated with an LC filter from the lower part the chassis which only supports the strong radiative common mode currents. In [118], a loop chip antenna does not excite strong currents in the upper part of the chassis of a clamshell/folder-type terminal. Another way is to use a balanced antenna (such as a bowtie) and totally isolate the chassis from the radiator structure [119]. This will, however, decrease the available impedance bandwidth, for example, compared to the antenna in Fig. 28 (2.4).

One possible solution to affect the current distribution is to use quarter-wavelength-long wavetraps which create a high-impedance location on the chassis and thus create a new wavemode, see Fig. 29a [120]. This solution with a 140-mm-long chassis is proposed by a Swedish research team [121]. The wavetraps are quarter-wavelength-long at 1.88 GHz. At the 1-GHz band the wavetraps as such would be physically unfeasibly long and hence this solution is limited to the upper band. Similar solution for a slider-type terminal has been proposed in [122]. The main problem of the wavetraps with 100-mm-long chassis in Fig. 29a is that they do not reduce the magnetic fields on the HAC plane since the strong currents in the wavetraps locally create very high magnetic fields, see Fig. 30a. In order to avoid both strong local electric and magnetic fields on the HAC plane, *inverted top* wavetraps are introduced in [**VIII**], see Fig. 29b. Compared to the case without the wavetraps in Fig. 28b, simulated electric and magnetic fields are both decreased up to 74% at 1.88 GHz on the HAC plane, see Fig. 30b. Across 1.85-1.91 GHz the electric and magnetic field values are decreased at least 63% and 66%, respectively. In addition to the remarkably reduced field strengths on the HAC plane, the impedance bandwidth is enhanced at the 2-GHz band the same way as in [120], and the head SAR value is also decreased 23% (from 0.83 W/kg to 0.64 W/kg, 1-g average maximum with

0.125-W input power) at 1.88 GHz since the wavetraps decrease the near fields on the head side, see Figs. 28b and 30b. The effect of the inverted-top wavetraps on the SAR values is later studied in [123] and [124].

A prototype based on the antenna structure shown in Fig. 29b was also designed, built and measured in [**VIII**] to validate the simulated results. The prototype had 6-dB return loss across 1.85-2.19 GHz (relative bandwidth 17%) and the total efficiency of 0.53 - 0.61 at 1.85-1.91 GHz. The 1-W normalised maximum electric and magnetic field values at 1.85 GHz (after the exclusion) are 81 V/m and 0.25 A/m, whilst the corresponding values of the reference prototype without the wavetraps are 290 V/m and 0.77 A/m.

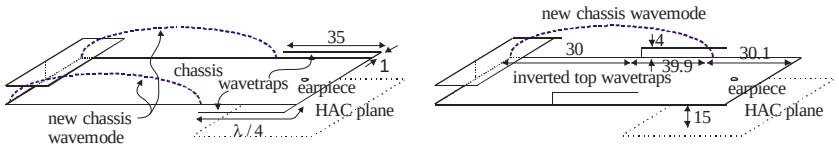

Fig. 29. a) Capacitive coupling element antenna structure and quarter-wavelength-long wavetraps at 1.88 GHz, and b) the idea of the inverted top wavetraps. Dimensions are in mm.

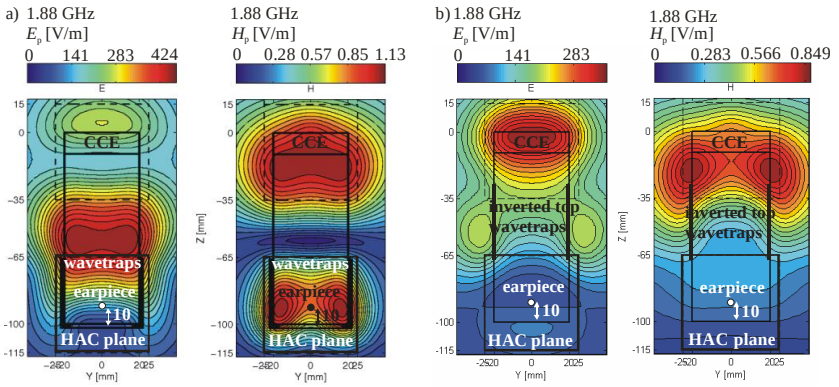

Fig. 30. Electric and magnetic fields of the full-metal antenna structure presented in a) Fig. 29a and b) Fig. 29b.

5 Summary of articles

[I] Broadband Equivalent Circuit Model for Capacitive Coupling Element –Based Mobile Terminal Antenna

It is shown how the behaviour of a capacitive coupling element (CCE)-based mobile terminal antenna can be modelled in the UHF band as a combination of the separate wavemodes of the structure. The agreement between the input impedances of the equivalent circuit model and EM-simulated antenna structure is excellent. The proposed equivalent circuit model improves the general understanding of the operation of the antenna structure. The model is used for analysing the combined performance of the capacitive coupling element and terminal chassis, but it also helps in analysing how different parts of the antenna structure contribute to the total impedance, bandwidth and radiation.

[II] Internal Broadband Antennas for Digital Television Receiver in Mobile Terminals

The implementation of internal broadband antennas for digital television receiver (DTV) in mobile terminals operating in the lower UHF band is studied in detail. Certain challenges such as inherently narrow impedance bandwidth of electrically small antennas and limited volume available for the antennas inside mobile terminals are identified and handled. The proposed design principle for DTV antennas is to decrease the total efficiency of the antenna to a level which is just good enough to ensure a sufficient signal-to-noise ratio and that way make the size of the antenna sufficiently small. The limits for the size of broadband capacitive coupling element-based DTV antenna structures inside handsets of different sizes are studied. The theoretical results suggest that the thinnest possible antenna element in today's typical-sized terminal is 9 mm when reserving 3 dB for the implementation losses. On the other hand, in tablet-sized terminals the antenna element can be made significantly thinner. In the end, a built prototype and simulated design are presented and compared with the theoretical limits studied in the paper. The results show that the studied antenna concept is a promising candidate for broadband DTV antennas in mobile terminals. The work also increases general understanding on the implementation of compact antennas in the lower UHF band. That is important, for instance, for the development of the antennas of low-band LTE and cognitive radio.

[III] Power loss and distortion minimization in tuning circuit for a mobile terminal antenna

Broadband tuning circuits of small antennas may have high power losses and/or high distortion if the designer does not pay attention to the placement of the lossy and nonlinear components in the circuit. Experimental results of the distortion of an SPDT HEMT switch under different impedance environments are presented. The results indicate that if the semiconductor switch is placed in the high-impedance environment, the distortion is higher than when it is placed in low-impedance environment. The results motivate a broadband frequency tuning circuit design for a mobile handset antenna. The tuning circuit, using HEMT switches and lumped reactances, compromises between reasonable power loss and distortion caused by the switching components. The design is simulated and prototyped for E-GSM900 and GSM1800 using a capacitive coupling element based antenna.

[IV] Mobile terminal antennas implemented by using direct coupling

The current trend in mobile terminals is an increasing number of systems. The volume occupied by the antennas of the radio systems is becoming more and more problematic and new low-volume antenna solutions are needed. Since the chassis of a mobile terminal operates as the main radiating structure, especially below 1 GHz, a very low-profile antenna structure can be achieved by using a direct feed, i.e., galvanically inducing currents on the surface of the chassis. The feed can be placed over an impedance discontinuity, for example, formed by a slot. Using this approach, an antenna structure for a small handheld digital television (DVB-H) receiver is presented. The realised gain of the antenna exceeds the specification by a 4-dB margin. The proposed antenna structure may also be used for multi-system terminals.

[V] Mobile terminal antennas implemented using optimized direct feed

A novel antenna structure based on optimised direct feed is presented. The antenna structure consists of the chassis of a mobile terminal, a feed structure and a matching circuitry. The chassis is cut in two pieces, which are connected with an inductor. The value of the inductor is tuned so that the lowest resonant frequency of the chassis equals the centre frequency of the operating band. The feed structure excites very strongly the resonant wavemode of the chassis and thus very large bandwidth (22% with 10 dB

return loss) is available. The feed structure can be integrated, for instance, on the PCB of a mobile terminal and thus the antenna is very low-profile. The antenna structure has been demonstrated with a simulated and measured prototype that covers the GSM850/900 and GSM1800/1900/UMTS systems.

[VI] Equivalent Circuit Model–Based Approach on the User Body Effect of a Mobile Terminal Antenna

The user body effect on the operation of mobile terminal antennas is investigated based on equivalent circuit modelling. The purpose is to increase the understanding of the phenomenon, which is important, for example, when designing mobile terminal antennas with minimised user body effect. The proposed circuit model can explain on a qualitative level the behaviour of the impedance and efficiency of UHF-band mobile terminal antennas caused by the lossy dielectric material located in the reactive near field of a mobile terminal antenna.

[VII] Effect of the User on the Operation of Lower UHF Band Mobile Terminal Antennas: Focus on Digital Television Receiver

This article deals with the effect of the user's hands on the performance of lower UHF-band antennas in handheld terminals. It is studied how the input impedance, efficiency and far field directional pattern of the internal broadband digital television (DTV) antenna are affected by the presence of the user's hands. The main part of the study has been carried out by applying FDTD simulations. Measurements have been performed to support the results obtained by simulations. In the worst case occur when the hand is close to the antenna element, and in that case as much as 7-11 dB decrease of the antenna efficiency compared to free space case is shown. The results also indicate that the power absorption to the hand(s) is generally a more severe problem for the total efficiency than the change of the matching. On the other hand, it is also shown that in certain cases the total efficiency of the antenna can even be improved due to the hands of the user. The results of this paper increase the understanding of the effect of the user's hands on the operation of the lower UHF-band antennas whose operation is based on the radiation of a finite ground plane.

[VIII] Near Field Control of Handset Antennas Based on Inverted Top Wavetraps: Focus on Hearing-aid Compatibility

The local reduction of the near fields is especially important for the operation of the possible hearing aid of the user. It is shown that inverted top wavetraps, which are quarter-wavelength-long resonators, can be used to control the near fields of a mobile terminal antenna. The reshaping of the near fields may also enable reduced specific absorption rate (SAR) values.

6 Conclusions

In this thesis, selected compact UHF-band antennas of mobile terminals are investigated in detail. The main goal was to understand the operation, benefits and challenges of the compact coupling-based antennas, whose operation is based on exploiting the separate wavemodes of the chassis as the main radiator. The antenna element itself can be made compact since it functions mainly as a coupler which couples to those chassis wavemodes. These kinds of antennas play an important role when implementing sufficiently small and thin antennas within handheld multi-system radios, where the volume reserved for antennas is very limited.

This work includes equivalent circuits for modelling the operation of coupling-based antennas [**I**], [**VI**], novel antenna implementations and their comprehensive operation analysis [**II**], [**III**], [**VII**], and new antenna inventions [**IV**], [**V**], [**VIII**]. The new solutions and understanding can be exploited in the development of the antennas for the multi-system handheld devices of the future.

The proposed equivalent circuit model provides improved general understanding of the operation of capacitive coupling element (CCE) antennas, as well as a tool for analysing the effect of each part of the antenna structure on the total impedance and radiation. The circuit model has also been modified to take into account the effect of lossy dielectric material on each wavemode, and then the model is used to explain the effect of the user on the impedance and efficiency behaviour of mobile terminal antennas.

The implementation, design and user effect of lower UHF-band (below 1 GHz) broadband antennas based on the CCE is studied in detail. The design principle of such receiving antennas is to sacrifice the performance (efficiency) of the antenna to the lowest acceptable level in order to implement the required impedance bandwidth with a sufficiently small and low-profile CCE. The shape and location of the CCE was designed to optimally excite the dominant wavemode of the chassis. In addition, optimal multi-resonant matching circuits with up to two additional resonators, consisting of high-Q lumped elements, were applied. Further increase of the number of the additional resonators, which might not anyway be feasible in practice, would not significantly increase bandwidth anymore (Bode-Fano theory). Thus, the bandwidths of the studied antenna structures approach the upper limit achievable with passive solutions. In particular, the lower limit for the size of selected CCE-based antenna

structures embedded within terminals of different sizes was studied. The results indicate that in today's small- and typical-size terminals relatively thick and large CCEs are required to provide the required performance (for the DVB-H system) in the lower UHF band. On the other hand, in tablet-size terminals the CCE can be made significantly thinner and smaller. Generally, the size of the chassis has a significant effect on the required size of the antenna element. The same method could be extended to evaluate the required sizes of CCEs in other frequency bands, such as low-band LTE and 1-GHz cellular systems. The user's hand very close to the CCE was shown to cause a large influence on the antenna operation among the studied hand grips. In that case, the total efficiency decreases significantly, mainly due to the absorption of the hand (not the mismatching). When the hand is located far from the CCE, it is not difficult to keep the performance up and actually, in certain cases it was shown that the hand can even improve the total efficiency of mobile terminal antennas. All these user effect results were explained on a qualitative level also with the help of the proposed equivalent circuit model.

Since the upper limit of the available impedance bandwidth is approached with the studied passive CCE antenna structures in the lower UHF band, ever larger virtual bandwidths and/or several separate non-simultaneous frequency bands can be covered with a single CCE only by using frequency-tuneable matching circuits. It has been studied in detail that the main challenges in the implementation of such tuning circuits are the resistive losses and non-linearity of the required RF semiconductor tuning component. The results show that the problems in the tuning component can be reduced by carefully designing the impedance environment of the semiconductor component. In the future, the expected development of the RF tuning components, such as MEMS switches, semiconductor switches and varactors, improves the feasibility of the wideband frequency-tuneable antennas.

It was demonstrated that very low-profile antennas can be implemented by exciting the chassis wavemodes galvanically with a direct feed across an impedance discontinuity, such as a slot which supports transmission-line-type (differential-type) wavemode. The coupling from the slot wavemode to the chassis major axis (common mode) wavemodes becomes relatively strong (compared to CCE antennas) and relatively large impedance bandwidths were achieved. The results also show that the main challenges with the direct feed antennas are related to the increased local specific absorption rate values and the complexity of the integration of the slots on the PCB of a real terminal.

This work also reveals several research topics that should be further studied in the future. Even though the implementation of the compact coupling-based antenna structures is well-understood, novel circuit technologies could still improve bandwidth-to-volume ratio, lower the resistive losses, and enable a higher integration level. Especially, methods for controlling or adjusting the electrical properties of the chassis could further improve the impedance bandwidth and thus enable ever smaller antenna elements. In the case of frequency-tuneable antennas, more flexible tuning range, lower resistive losses and distortion would be important features of the antennas of the mobile terminals of the future, and they should be improved in the further studies. The enhancement of the isolation between dual or multiple antenna elements, especially in the lower UHF band, requires more work with the antenna structures as well as on the circuit/filter level. In addition, in the case of frequency-tuneable antennas, the filtering/decoupling might also need to be frequency-tuneable. Hence, the development of the circuit technologies is in key position in the improvement of small mobile terminal antennas in the future. More work with the SAR control methods of the direct feed antennas is also required. The future work on the effect of the user on the operation of the antenna could include research in the compensation methods, for instance, using multi-element technology.

References

[1] P. Vainikainen, J. Holopainen, C. Icheln, O. Kivekäs, M. Kyrö, M. Mustonen, S. Ranvier, R. Valkonen, and J. Villanen, "More Than 20 Antenna Elements in Future Mobile Phones, Threat or Opportunity?," *EuCAP 2009 3rd European Conference on Antennas & Propagation*, Berlin, Germany, 23-27 March 2009.

[2] P. Gardner, R. Hamid, P. S. Hall, J. Kelly, F. Ghanem, and E. Ebrahimi, "Reconfigurable antennas for cognitive radio: Requirements and potential design approaches," *IET Seminar on Wideband/Multiband Antennas and Arrays for Civil or Defence Applications*, London, 13 March 2008.

[3] K. Fujimoto, A. Henderson, K. Hirasawa and J. R. James, *Small antennas*, New York, 1987, Research Studies Press, 300 p.

[4] A. V. Räisänen and A. Lehto, *Radio Engineering for Wireless Communication and Sensor Applications*, Artech House (Boston, Massachusetts), May 2003, 366 p.

[5] A. D. Yaghjian and S. R. Best, "Impedance, bandwidth, and Q of antennas," *IEEE Transactions on Antennas and Propagation*, vol. 53, no. 4, Apr. 2005, pp. 1298–1324.

[6] L. J. Chu, "Physical limitations on omni-directional antennas," *Journal of Appl. Physics*, vol. 19, 1948, pp. 1163-1175.

[7] R. C. Hansen, "Fundamental Limitations in Antennas," *Proceedings of the IEEE*, Vol. 69, No. 2, February 1981, pp. 170-182.

[8] J. S. McLean, "A Re-Examination of the Fundamental Limits on the Radiation Q of Electrically Small Antennas," *IEEE Transactions on Antennas and Propagation*, Vol. 44, No. 5, May 1996, pp. 672-676.

[9] H.F. Pues and A.R. van de Capelle, "An impedance-matching technique for increasing the bandwidth of microstrip antennas," *IEEE Transactions on Antennas and Propagation*, Vol. 37, No. 11, November 1989, pp 1345-1354.

[10] IEEE, *IEEE Standard Definitions of Terms for Antennas*, IEEE STD-145, 1993.

[11] E. S. Kuh, R. A. Rohrer, *Theory of Linear Active Networks*, San Francisco, California, 1967, Holden-Day, Inc.

[12] J. D. Kraus, R.J. Marhefka, *Antennas for All Applications, Third Edition*, McGraw-Hill, New York, 2002, pp. 938.

[13] D. M. Pozar, *Microwave Engineering*, John Wiley Sons, Inc., 1998, 716 p.

[14] International Commission on Non-Ionizing Radiation Protection (ICNIRP), "Guidelines for limiting exposure to time-varying electric, magnetic, and electromagnetic fields (up to 300 GHz)," *Health Physics*, vol. 74, no. 4, April 1998, pp. 494-522.

[15] ANSI/IEEE Std C95.1, 1999 Edition, *IEEE Standard for Safety Levels with Respect to Human Exposure to Radio Frequency Electromagnetic Fields, 3 kHz to 300 GHz*, New York, USA, April 1999, 73 p.

[16] *American National Standard for Method of Measurements of Compatibility Between Wireless Communication Devices and Hearing Aids*, ANSI C63.19-2007, Amer. Nat. Standards Inst., New York, 2007.

[17] G. L. Matthaei, L. Young, and E. M. T. Jones, *Microwave Filters, Impedance Matching Networks and Coupling Structures*, McGraw-Hill, New York, 1964.

[18] J. Ollikainen, *Design and implementation techniques of wideband mobile communication antennas*, Doctoral thesis, Helsinki University of Technology, Radio Laboratory, Espoo, Finland, November 2004 [Online]. Available: http://lib.tkk.fi/Diss/2004/isbn9512273810/ (cited 17.8.2010).

[19] H. W. Bode, *Network Analysis and Feedback Amplifier Design*, Van Nostrad, N.Y., 1945.

[20] R. M. Fano, "Theoretical Limitation on the Broad-Band Matching of Arbitrary Impedances," *Journal of the Franklin Institute*, vol. 249, January 1950 pp. 57-83, and February 1950, pp. 139-154.

[21] J. Villanen, P. Vainikainen, "Optimum Dual-resonant Impedance Matching of Coupling Element Based Mobile Terminal Antenna Structures," *Microwave and Optical Technology Letters*, Vol. 49, No. 10, October 2007, pp. 2472-2477.

[22] Pat. WO 2007/036774 (A1), *Dual-resonant antenna*, Nokia Corporation, Espoo, Finland, (T. Ranta), Appl. 29.8.2006, granted 5.4.2007, pp. 27.

[23] M. Komulainen, M. Berg, H. Jantunen, E. Salonen, "Compact varactor-tuned meander line monopole antenna for DVB-H signal reception," *Electronic Letters*, Vol. 43, no. 24, November 2007, pp. 1324-1326.

[24] L. Huang and P. Russer, "Electrically Tuneable Antenna Design Procedure for Mobile Applications," *IEEE Transactions on Microwave Theory and Techniques*, Vol. 56, No. 12, December 2008, pp. 2789-2797.

[25] Z. H. Hu, C. T. P. Song, J. Kelly, P. S. Hall, and P. Gardner, "Wide tuneable dual-band reconfigurable antenna," *IET Electronics Letters*, Volume 45, Issue 22, October 22, 2009, p.1109–1110.

[26] Pat. FI114260, *Modular coupling structure for a radio device and a portable radio device*, P. Vainikainen, J. Ollikainen, O. Kivekäs, and I. Kelander, Finland, Appl. 20002529, 17.11.2000, (15.09.2004), 22 p.

[27] J. Villanen, M. Mikkola, C. Icheln, and P. Vainikainen, "Radiation characteristics of antenna structures in clamshell-type phones in wide frequency range," *Proceedings of the 65th IEEE Vehicular Technology Conference (VTC2007-spring)*, Dublin, Ireland, April 2007, CD-ROM (ISBN 1-4244-0266-2), pp. 382-386.

[28] J. Holopainen, *Antenna for Handheld DVB Terminal*, Master's thesis, Helsinki University of Technology, Radio Laboratory, Espoo, Finland, May 2005.

[29] R. Valkonen, *Broadband Tuning of Small Antennas*, Master's thesis, Helsinki University of Technology, Radio Laboratory, Espoo, Finland, March 2007.

[30] R. Valkonen, J. Holopainen, C. Icheln, and P. Vainikainen, "Broadband tuning of mobile terminal antennas", *EuCAP 2007 2nd European Conference on Antennas & Propagation*, Edinburgh, UK, 11-16 November 2007, CD-ROM (9-7808-6341-8426), paper: tu2.6.6.pdf.

[31] O. Kivekäs, J. Ollikainen, and P. Vainikainen, "Frequency-tuneable internal antenna for mobile phones," *Proceedings of the 12th International Symposium on Antennas (JINA 2002)*, Nice, France, Nov. 12-14, 2002, vol. 2, pp. 53-56.

[32] C. A. Balanis, *Modern Antenna Handbook*, New York, 2008, John Wiley & Sons, 1680 p.

[33] O. Kivekäs, *Design of high-efficiency antennas for mobile communication devices*, Doctoral thesis, Helsinki University of Technology, Radio Laboratory, Espoo, Finland, August 2005 [Online]. Available: http://lib.tkk.fi/Diss/2005/isbn9512277581/

[34] "Test Plan for Mobile Station Over the Air Performance: Method of Measurement for Radiated RF Power and Receiver Performance," CTIA Certification, Technical report, Revision 3.0, April 2009.

[35] OTA Hand Phantoms, Monoblock phone grip SHO V2RB/LB, Fold phone grip SHO V2RC/LC, Narrow data grip SHO V2RD/LD, PDA grip SHO V2RP/LP, Schmid & Partner Eng. AG, Zurich, Switzerland, 2010 [Online]. Available: http://www.speag.com/ (cited 3.9.2010).

[36] CTIA Phantom Hand Family, Monoblock phone grip IXB-050R, Fold phone grip IXB-051R, Narrow data grip IXB-052R, PDA grip IXB-053R, IndexSAR, Ltd. Surrey, UK [Online]. Available: http://www.indexsar.com/ (cited 3.9.2010).

[37] C. A. Balanis, Antenna Theory: Analysis *and Design*, 2. Edition, New York, 1997, John Wiley & Sons, 941 p.

[38] T. Taga, "Analysis of planar inverted-F antennas and antenna design for portable radio equipment," in *Analysis, Design and Measurement of Small and Low-Profile Antennas*, K. Hirasawa and M. Haneishi, Eds. Norwood, MA: Artech House, 1992, ch. 5, pp.161-180.

[39] K. L. Wong, "Planar Antennas for Wireless Communication," John Wiley & Sons Inc., Hoboken, New Jersey, USA, 2003, 301 p.

[40] Z. Li and Y. Rahmat-Samii, "Optimization of PIFA–IFA combination in handset antenna designs," *IEEE Transactions on Antennas and Propagation*, Vol. 53, No. 5, May 2005, pp. 1770–1778.

[41] J. Villanen, *Miniaturization and evaluation methods of mobile terminal antenna structures*, Doctoral thesis, Helsinki University of Technology, Radio Laboratory, Espoo, Finland, November 2007 [Online]. Available: http://lib.tkk.fi/Diss/2007/isbn9789512289646// (cited 3.9.2010).

[42] "Mobile and Portable DVB-T/H Radio Access - Interface Specification," EICTA, Technical report, version 2.0, 2007.

[43] "DVB-H Implementation Guidelines," DVB Project, DVB Document A092, Technical report, Rev. 2 May 2007.

[44] T. Asunmaa, *Sisäinen käsipuhelinantenni* (*Internal handset antenna*), Master's thesis, Helsinki University of Technology, Radio Laboratory, Espoo, Finland, February 2001.

[45] C. W. Yang, C. W. Jung, "Broad dual-band PIFA using self-complementary structure for DVB-H applications," *Electronics Letters*, vol. 46, no. 9, April 2010, pp. 606 – 608.

[46] D. Manteuffel, M. Arnold, "Considerations for Reconfigurable Multi-Standard Antennas for Mobile Terminals," *Proceedings of IEEE iWAT 2008 Small Antennas and Novel Metamaterials*, Chiba, Japan, 2008, paper: P127.

[47] R. E. Collin, *Antennas and Radiowave Propagation*, McGraw-Hill, New York, 1985, pp. 293-336.

[48] B. S. Collins, "Small Antennas for the Reception of Future Mobile Television Services," *Proceedings of IEEE iWAT 2009 Small Antennas and Novel Metamaterials*, Santa Monica, California, USA, March 2009, paper: 1569175875.pdf.

[49] Z. D. Milosavljevic, "A Varactor-Tuned DVB-H Antenna," *IEEE iWAT 2007 Small Antennas and Novel Metamaterials*, Cambridge, UK, March 2007, pp. 124-127.

[50] J. Holopainen, J. Villanen, M. Kyrö, C. Icheln and P. Vainikainen, "Antenna for handheld DVB terminal", *Proceedings of IEEE iWAT 2006 Small Antennas and Novel Metamaterials*, White Plains, New York, USA, 6-9 March 2006, CD-ROM (ISBN 0-7803-9444-5), p077.

[51] R. Li, B. Pan, J. Papapolymerou, J. Laskar, M. Tentzeris, "Low-Profile Broadband Planar Antennas for DVB-H, DCS-1800, and IMT-2000 Applications," *2007 IEEE AP-S International Symposium on Antennas and Propagation*, Honolulu, Hawaii, June 10-15, 2007.

[52] J.-K. Wee, J. W. Park, I. S. Yeom, B.-G. Kim, and C. W. Jung, "Compact DVB-H Antenna With Broad Dual-Band Operation for PMP Applications", *IEEE Antennas and Wireless Propagation Letters,* vol. 9, 2010, pp. 580-583.

[53] K.-L. Wong, Y.-W. Chi, B. Chen and S. Yang, "Internal DTV antenna for folder-type mobile phone," *Microwave and Optical Technology Letters*, vol.48, no.6, June 2006, pp. 1015-1019.

[54] H. Rhyu, C. Jung, J. Byun, M. Park, Y. Chung, T. Kim, and B. Lee, "DVB-H Antenna Design Using Folder-Type Chassis and Coupling Element on a Ferrite," *IEEE Antennas and Wireless Propagation Letters,* vol. 8, 2009, pp. 453-456.

[55] J.-N. Lee, J.-K. Park, and J.-S. Kim, "Design of the DVB-H Antenna Using the Coupling Concept," *Proceedings of the 39th European Microwave Conference,* Rome, Italy, 29 September - 1 October, 2009, pp. 532-535.

[56] P. Vainikainen, J. Ollikainen, O. Kivekäs, and I. Kelander, "Resonator-based analysis of the combination of mobile handset antenna and chassis," *IEEE Transactions on Antennas and Propagation*, Vol. 50, No. 10, October 2002, pp. 1433-1444.

[57] J. Villanen, J. Ollikainen, O. Kivekäs, and P. Vainikainen, "Coupling element based mobile terminal antenna structures," *IEEE Transactions on Antennas and Propagation*, vol. 54, no. 7, pp. 2142 - 2153.

[58] W. L. Schroeder, A. A. Vila, and C. Thome, "Extremely small, wide-band mobile phone antennas by inductive chassis mode coupling," *Proc. 36th European Microwave Conference (EuMC'06)*, Manchester, UK, September 2006, pp. 1702-1705.

[59] J. Villanen, *Compact antenna structure for mobile handsets*, Master's thesis, Espoo, Helsinki University of Technology, February 2003, 83 p.

[60] R. F. Harrington and J. R. Mautz, "Theory of characteristic modes for conducting bodies," *IEEE Transactions on Antennas and Propagation*, vol. 19, no. 5, pp. 622-628, September 1971.

[61] M. Cabedo-Fabres, E. Antonino-Daviu, M. Ferrando-Bataller, and A. Valero-Nogueira, "On the use of characteristic modes to describe patch antenna performance," *Proc. IEEE Antennas and Propagation Society International Symposium Digest*, Columbus (Ohio), USA, June 2003, pp. 712-715.

[62] C. T. Famdie, W. L. Schroeder and K. Solbach, "Numerical Analysis of Characteristic Modes on the Chassis of Mobile Phones", *EuCAP 2006 1st European Conference on Antennas and Propagation,* Nice, France, Nov. 6-10, 2006.

[63] T. Taga, K. Tsunekawa, "Performance analysis of a build-in planar inverted F antenna for 800 MHz band portable radio units," *IEEE Journal of Selected Areas in Communications*, Vol. 5, no. 5, pp. 921-929, June 1987.

[64] O. Kivekäs, J. Ollikainen, T. Lehtiniemi, and P. Vainikainen, "Bandwidth, SAR, and efficiency of internal mobile phone antennas," *IEEE Transactions on Electromagnetic Compatibility*, vol. 46, no. 1, Feb. 2004, pp. 71-86.

[65] J. Rahola, J. Ollikainen, "Optimal antenna placement for mobile terminals using characteristic wavemodes," *EuCAP 2006 1st European Conf. Antennas Propag.,* Nice, France, Nov. 6-10, 2006.

[66] E. Antonino-Daviu, M. Cabedo-Fabres, M. Ferrando-Bataller, and J. Herranz-Herruzo, "Analysis of the coupled chassis-antenna modes in mobile handsets," *Proc. IEEE Antennas and Propagation Society International Symposium Digest*, Monterey (California), USA, June 2004, pp. 2751-2754.

[67] C. T. Famdie, W. L. Schroeder, K. Solbach, "Optimal antenna location on mobile phones chassis based on the numerical analysis of characteristic modes", *Proceedings of the 37th European Microwave Conference, EuMC2007*, Munich, Germany, October 2007, pp. 987 - 990.

[68] J. Villanen, J. Poutanen, C. Icheln, and P. Vainikainen, "A wideband study of the bandwidth, SAR and radiation efficiency of mobile terminal antenna structures," *Proceedings of IEEE iWAT 2007 Small Antennas and Novel Metamaterials*, Cambridge, UK, March 2007, pp. 49-52.

[69] J. Poutanen, J. Villanen, C. Icheln, and P. Vainikainen, "Behavior of mobile terminal antennas near human tissue at a wide frequency range," *Proceedings of IEEE iWAT 2008 Small Antennas and Novel Metamaterials*, Chiba, Japan, 2008, paper: P123.

[70] IE3D, a method of moments based commercial electromagnetic simulator, ver. 12.2, Zeland Software, Inc., Fremont, California, USA [Online]. Available: http://www.mentor.com/electromagnetic-simulation/ (cited 15.9.2010).

[71] J. Villanen, J. Holopainen, O. Kivekäs, and P. Vainikainen, "Mobile broadband antennas," *URSIGA 2005 conference,* New Delhi, India, October 2005, file BC.2(01464).pdf.

[72] J. Villanen, C. Icheln, and P. Vainikainen, A coupling element-based quad-band antenna structure for mobile terminals, *Microwave and Optical Technology Letters*, vol. 49, no. 6, pp. 1277-1282, June 2007.

[73] U. Bulus, K. Sohlbach, "Modelling of the Monopole Interaction With a Small Chassis," *EuCAP 2009 3rd European Conf. Antennas Propag.,* Berlin, Germany, March 23-27, 2009.

[74] P. S. Hall, P. Gardner, J. Kelly, E. Ebrahimi, M.R. Hamid, and F. Ghanem, "Antenna Challenges in Cognitive Radio," *ISAP 2008 International Symposium on Antennas and Propagation*, Taipei, Taiwan, 27-30 October 2008, paper: 1645173.pdf.

[75] K. R. Boyle, "Mobile phone antenna performance in the presence of people and phantoms," *IEE Technical Seminar Antenna Meas. and SAR (AMS 2002)*, Loughborough University, UK, 2002, 4 p.

[76] K. R. Boyle, "The performance of GSM 900 antennas in the presence of people and phantoms," *Proc. 12th International Conference on Antennas and Propagation (ICAP 2003)*, Exeter, UK, 2003, pp. 35-38.

[77] Rogers RT Duroid 5870 high frequency laminate, thickness 0.8 mm [Online]. Available: http://www.rogerscorp.com/ (cited 10.8.2010).

[78] Murata products [Online]. Available http://www.murata.com/products/index.html (cited 10.8.2010).

[79] J. Rahola, "Bandwidth potential and electromagnetic isolation: Tools for analysing the impedance behaviour of antenna systems," *EuCAP 2009 3rd European Conf. Antennas Propag.*, Berlin, Germany, March 23-27, 2009.

[80] DVB-H EU 470-750 MHz Planar PWB Antenna, Pulse part number W3510, [Online]. Available: http://www.pulseeng.com (cited 10.8.2010).

[81] R. Valkonen, C. Luxey, J. Holopainen, C. Icheln, P. Vainikainen, "Frequency-reconfigurable mobile terminal antenna with MEMS switches," *EuCAP 2010 4th European Conference on Antennas & Propagation* 2010, 12-16 April 2010, Barcelona, Spain.

[82] G. M. Rebeiz, *RF MEMS: Theory, Design, and Technology*. Hoboken, NJ: Wiley, 2003.

[83] P. Grant and M. Denhoff, "A comparison between RF MEMS switches and semiconductor switches." *Proceedings of the 2004 International Conference on MEMS, NANO and Smart Systems (ICMENS04)*, Alberta, Canada, Aug. 25-27 2004, pp. 515–521.

[84] Z. Liu, K. Boyle, J. Krogerus, M. de Jongh, K. Reimann, R. Kaunisto, J. Ollikainen, "MEMS-Switched, Frequency-Tunable Hybrid SLOT/PIFA Antenna," *IEEE Antennas and Wireless Propagation Letters*, vol. 8, May 2009, pp. 311-314.

[85] C. T. P. Song, Z. H. Hu, J. Kelly, P. S. Hall, and P. Gardner, "Wide tuneable dual-band reconfigurable antenna for future wireless devices", *Loughborough Antennas and Propagation Conference, Loughborough, UK,* 16-17 November, 2009.

[86] Z. H. Hu, J. Kelly, C. T. P. Song, P. S. Hall, and P. Gardner, "A Novel Wide Tuneable Dual-Band Reconfigurable Chassis-Antenna for Future Mobile Terminals", *EuCAP 2010, European Conference on Antennas and Propagation,* Barcelona, Spain, 12-16 April 2010.

[87] D. Manteuffel, M. Arnold, Y. Makris, Z.-N. Chen, “Concepts for Future Multistandard and Ultra Wideband Mobile Terminal Antennas using Multilayer LTCC Technology,“ *Proceedings of IEEE iWAT 2009 Small Antennas and Novel Metamaterials*, Santa Monica, California, USA, March 2009, paper: 1569175881.pdf.

[88] U. Bulus, C. T. Famdie, K. Solbach, ”Equivalent-Circuit Modelling of Chassis Radiator,” *German Microwave Conference, GeMIC 2009*, Munich, Germany, 16-18 March, 2009.

[89] J. D. Kraus, *Antennas*, 2. Edition, New York, 1988, McGraw-Hill, 892 pp.

[90] R. Valkonen, J. Poutanen, J. Holopainen, C. Icheln, and P. Vainikainen, "Effects of Nearby Metallic Patches on an Antenna Based on Segmented Mobile Terminal Chassis", *EuCAP 2009 3rd European Conference on Antennas & Propagation*, Berlin, Germany, 23-27 March 2009.

[91] M. Cabedo-Fabres, E. Antonino-Daviu, A. Valero-Nogueira, and M. Ferrando-Bataller, “Wideband radiating ground plane with notches,” *Proc. IEEE Antennas and Propagation Society International Symposium Digest*, Washington, USA, July 2005, pp. 560-563.

[92] W. L. Schroeder, A. A. Vila, and C. Thome, “Extremely Small, Wide-band Mobile Phone Antennas by Inductive Chassis Mode Coupling,” *Proceedings of the 36th European Microwave Conference, EuMC 2006*, Manchester, UK, 10-15 September, 2006.

[93] A. Zhao, “Wideband and low-profile antenna by using a unique direct feed approach,” *IEEE Electrical Design of Advanced Packaging & Systems Symposium, EDAPS 2009,* Singapore, December 7-9, 2009.

[94] A. Zhao, “Wideband and low-profile antenna for mobile terminals,” *Microwave and Optical Technology Letters*, vol. 52, no. 12, pp. 2724-2728, December 2010.

[95] “Small Antenna Contest Report,” Antenna Center of Excellence (ACE) deliverable, report, 31.12.2007.

[96] J. Ollikainen and P. Vainikainen, *Design and bandwidth optimization of dual-resonant patch antennas*, Helsinki University of Technology, Radio Laboratory publications, Report S 252, Espoo 2002, Finland, 41 p.

[97] J. Holopainen, *Handheld DVB and Multisystem Radio Antennas*, Licentiate thesis, Helsinki University of Technology, Department of Radio Science and Engineering, Espoo, Finland, April 2008 [Online]. Available: http://lib.tkk.fi/Lic/2008/urn011818.pdf (cited 14.10.2010).

[98] J. Holopainen, J. Poutanen, C. Icheln, and P. Vainikainen, ”User effect of antennas for handheld DVB terminal”, *IEEE ICEAA 2007 International Conference on Electromagnetics in Advanced Applications*, Turin, Italy, 17-21 September 2007, CD-ROM (1-4244-0767-2), paper: 313.pdf.

[99] Pat. WO2008/120038 (A1), “An antenna arrangement”, Nokia Corporation, Espoo, Finland, (J. Ollikainen, J. Villanen, J. Holopainen, C. Icheln, and P. Vainikainen), Appl. 30.3.2007, granted 10.9.2008, pp. 22.

[100] J. Toftgård, S. N. Hornsleth, ”Effects on Portable Antennas of the Presence of a Person,” *IEEE Transactions on Antennas and Propagation*, vol. 41, No. 6, June 1993.

[101] K. R. Boyle, “The Performance of GSM 900 Antennas in the Presence of People and Phantoms,” in *Proc. 12th Int. Conf. Antennas and Propagation (ICAP 2003)*, Exeter, U.K., Mar. 31–Apr. 3 2003, vol. 1, pp. 35–38.

[102] C.-M. Su, C.-H. Wu, K.-L. Wong, S.-H. Yeh, C.-L. Tang, “User’s hand effects on EMC internal GSM/DCS dual-band mobile phone antenna,” *Microwave and Optical Technology Letters*, vol. 48, issue 8, May 2006, pp. 1563-1569.

[103] K. R. Boyle, Y. Yuan, L. P. Ligthart, “Analysis of Mobile Phone Antenna Impedance Variations with User Proximity,” *IEEE Transactions on Antennas and Propagation*, vol. 55, issue 2, February 2007, pp. 364-372.

[104] K.-L. Wong, Y.C. Lin, and B. Chen, “Internal patch antenna with a thin air-layer substrate for GSM/DCS operation in a PDA phone,” *IEEE Transactions on Antennas and Propagation*, vol. 55, No. 4, April. 2007, pp. 1165-1172

[105] T. Huang, K. R. Boyle, ”User Interaction Studies on Handset Antennas,” *EuCAP ’07, The Second European Conference on Antennas and Propagation*, 11-16 November 2007, Edinburg, UK.

[106] R. F. Harrington, *Time-Harmonic Electromagnetic Fields*. NewYork: McGraw-Hill, 1961, pp. 317–380.

[107] M. Pelosi, O. Franek, M. B. Knudsen, M. Christensen, G. F. Pedersen, ”A grip study for Talk and Data Modes in Mobile Phones,” *IEEE Transactions on Antennas and Propagation,* vol. 57, No. 4, April 2009.

[108] P. Hui, “Positive Hand Effects on Mobile Handset Antennas,” *APMC 2008, Asia-Pacific Microwave Conference*, Macau, 16-20 December, 2008.

[109] P. Ramachandran, Z. D. Milosavljevic, C. Beckman, “Adaptive Matching Circuitry for Compensation of Finger Effect on Handset Antennas,” *EuCAP 2009 3rd European Conference on Antennas and Propagation*, Berlin, Germany, March 23-27, 2009, pp. 801-804.

[110] K. Boyle, T. Bakker, M. de Jongh, A. van Bezooijen, “Real-time Adaption of Mobile Antenna Impedance Matching,” *IEEE Loughborough Antennas & Propagation Conference 2010,* Loughborough, UK, 8-9 November 2010, pp. 22-25.

[111] M. Kyrö, M. Mustonen, C. Icheln, and P. Vainikainen, “Dual-element antenna for DVB-H terminal,” *LAPC 2008 Loughborough Antennas & Propagation Conference*, Loughborough, UK, 17-18 March, 2008.

[112] R. Valkonen, S. Myllymäki, A. Huttunen, J. Holopainen, J. Ilvonen, P. Vainikainen, and H. Jantunen, “Compensation of finger effect on a mobile terminal antenna by antenna selection,” in *2010 International Conference on Electromagnetics in Advanced Applications (ICEAA'10 Offshore)*, Sydney, Australia, September 20-24, 2010, pp. 364-367.

[113] S. M. Ali, G. Huanhuan, “Chassis wavemode effects on hearing aid compatibility at 900 MHz,” 2010 *IEEE AP-S International*

Symposium on Antennas and Propagation, Toronto, Canada, 11-17 July 2010.

[114] S. M. Ali, H. Gu, "Effects of Chassis Currents on Hearing Aids Compatibility in the Handsets," *IEEE Transactions on Electromagnetic Compatibility*, vol. 52, no. 4, November 2010, pp. 837-842.

[115] T. Yang, W. A. Davis, W. L. Stutzman, and M.-C. Huynh, "Cellular-Phone and hearing-aid interaction: An antenna solution," *IEEE Antennas Propagation Magazine*, vol. 50, no. 3, Jun. 2008, pp. 51–65.

[116] P. Hui, "Near fields of phased antennas for mobile phones," *APMC 2009, Asia Pacific Microwave Conference,* 7-10 December 2009, Singapore.

[117] A. Zhao, J. Ollikainen, J. Thaysen, T. Bodvarsson, "A novel approach to reduce the near field electromagnetic scattering for designing HAC compatible mobile phones," *Microwave and Optical Technology Letters*, vol. 52, no. 3, March 2010, pp. 709-715.

[118] W.-Y. Li, K.-L. Wong, C.-Y. Wu, "Hearing Aid-Compatible Loop Chip Antenna for Penta-Band Clamshell Mobile Phone Application," *APMC 2009, Asia Pacific Microwave Conference,* 7-10 December 2009, Singapore, pp. 2463-2466.

[119] J. Ilvonen, J. Holopainen, O. Kivekäs, R. Valkonen, C. Icheln, and P. Vainikainen, "Balanced antenna structures of mobile terminals," *EuCAP 2010, 4th European Conference on Antennas and Propagation,* Barcelona, Spain, 12-16 April 2010.

[120] P. Lindberg, E. Öjefors, "A Bandwidth Enhancement Technique for Mobile Handset Antennas Using Wavetraps, *IEEE Transaction on Antennas and Propagation*, Vol. 54, No. 8, August 2006, pp. 2226-2233.

[121] P. Lindberg, A. Kaikkonen, M. Südow, "Improvement of Hearing Aid Compatibility (HAC) of Terminal Antennas Using Wavetraps," *iWAT 2009 IEEE International Workshop on Antenna Technology*, Santa Monica, California, USA, 2-4 March 2009, paper: PS122.

[122] B. Bahramzy, L. Azzinnari, K. B. Jakobsen, M. Sager, "Near-Field Reduction Technique in the Speaker Area of Slide Mobile Phones for Improved HAC Performance," *2009 IEEE AP-S International Symposium on Antennas and Propagation*, Charleston, South Carolina, USA, June 1-5, 2009.

[123] M. R. Islam, M. Ali, "Elevation Plane Beam Scanning of a Novel Parasitic Array Radiator Antenna for 1900 MHz Mobile Handheld Terminals," *IEEE Transaction on Antennas and Propagation*, Vol. 58, No. 10, October 2010, pp. 3344-3352.

[124] M. R. Islam, M. Ali, "Ground Current Modification of Mobile Terminal Antennas and Its Effects," to be published in *IEEE Antennas and Wireless Propagation Letters,* vol. 10, 2011.

The background of this thesis is the trend of ever decreasing space available for antennas embedded within mobile terminals. At the same time the antennas are increasingly required to cover a large number of separate frequency bands and/or have wideband operation. In addition, those antennas should perform sufficiently well in the vicinity of the user. This forms the motivation for the novel compact coupling-based antennas introduced and studied in this thesis. The operation of such antennas is based on exploiting the wavemodes of the chassis of a mobile terminal as the main radiator. The antenna element itself functions mainly as a coupler which couples to those radiating chassis wavemodes. This work concentrates on the modelling, implementation and design of such antennas in free space, and the effect of the user on the operation of the antenna. The understanding gained in this thesis can be exploited in the development of the antennas for mobile terminals of the future.

ISBN: 978-952-60-4086-8 (pdf)
ISBN: 978-952-60-4085-1
ISSN-L: 1799-4934
ISSN: 1799-4942 (pdf)
ISSN: 1799-4934

Aalto University
School of Electrical Engineering
Department of Radio Science and Engineering
www.aalto.fi

BUSINESS + ECONOMY

ART + DESIGN + ARCHITECTURE

SCIENCE + TECHNOLOGY

CROSSOVER

DOCTORAL DISSERTATIONS

Aalto-DD 28/2011